Selective coupling of type 6 adenylyl cyclase with type 2 IP_3 receptors mediates direct sensitization of IP_3 receptors by cAMP

Stephen C. Tovey, Skarlatos G. Dedos, Emily J.A. Taylor, Jarrod E. Church, and Colin W. Taylor

Department of Pharmacology, Universsity of Cambridge, Cambridge CB2 1PD, England, UK

Interactions between cyclic adenosine monophosphate (cAMP) and Ca^{2+} are widespread, and for both intracellular messengers, their spatial organization is important. Parathyroid hormone (PTH) stimulates formation of cAMP and sensitizes inositol 1,4,5-trisphosphate receptors (IP_3R) to IP_3. We show that PTH communicates with IP_3R via "cAMP junctions" that allow local delivery of a supramaximal concentration of cAMP to IP_3R, directly increasing their sensitivity to IP_3. These junctions are robust binary switches that are digitally recruited by increasing concentrations of PTH. Human embryonic kidney cells express several isoforms of adenylyl cyclase (AC) and IP_3R, but IP_3R2 and AC6 are specifically associated, and inhibition of AC6 or IP_3R2 expression by small interfering RNA selectively attenuates potentiation of Ca^{2+} signals by PTH. We define two modes of cAMP signaling: binary, where cAMP passes directly from AC6 to IP_3R2; and analogue, where local gradients of cAMP concentration regulate cAMP effectors more remote from AC. Binary signaling requires localized delivery of cAMP, whereas analogue signaling is more dependent on localized cAMP degradation.

Introduction

Cells use a limited repertoire of diffusible intracellular messengers, including cAMP and Ca^{2+}, to regulate most aspects of their behavior, yet they succeed in responding appropriately to a barrage of extracellular signals. The versatility of intracellular messengers is increased by their precise spatial and temporal organization. Local increases in Ca^{2+} (Berridge, 1997) or cAMP (Zaccolo and Pozzan, 2002; Mongillo et al., 2006; Smith et al., 2006; Willoughby and Cooper, 2007) can selectively regulate closely associated proteins, whereas more global changes regulate different processes. Both Ca^{2+} and cAMP can also be delivered in precise temporal patterns (Berridge, 1997; Gorbunova and Spitzer, 2002; Dyachok et al., 2006). The frequencies of these messenger spikes are important in determining responses to Ca^{2+} (Dupont et al., 2003) and are also likely also to be important for cAMP spikes. The versatility of both messengers is increased further by interactions between them (Bruce et al., 2003; Werry et al., 2003; Screaton et al., 2004; Willoughby and Cooper, 2007). Ca^{2+}, for example, regulates cAMP formation and degradation, and by regulating protein kinases and calcineurin, it modulates many effects of protein kinase A (PKA). Conversely, cAMP regulates formation and phosphorylation of inositol 1,4,5-trisphosphate (IP_3), the activities of Ca^{2+} channels and pumps, and formation of other Ca^{2+}-mobilizing messengers. Such interactions endow cells with computational ability (Bray, 1995). Many proteins involved in cAMP and Ca^{2+} signaling exist in multiple isoforms, which may differ in behavior and expression. This diversity adds further to the complexity of the signaling pathways, but its physiological significance is incompletely understood.

Parathyroid hormone (PTH) plays a central role in the regulation of plasma Ca^{2+} concentration, although its receptors are also expressed in tissues unrelated to Ca^{2+} homeostasis. Each of

S.C. Tovey, S.G. Dedos, and E.J.A. Taylor contributed equally to this paper.

Correspondence to Colin W. Taylor: cwt1000@cam.ac.uk

Abbreviations used in this paper: AC, adenylyl cyclase; AKAP, A kinase–anchoring protein; CCh, carbachol; CNGC, cyclic nucleotide-gated cation channel; DDA, 2′,5′-dideoxyadenosine; epac, exchange protein activated by cAMP; FK, forskolin; HBS, Hepes-buffered saline; HEK, human embryonic kidney; HEK-PR1, HEK cells stably expressing human type I PTH receptors; IBMX, 3-isobutyl-1-methylxanthine; IP, immunoprecipitation; IP_3, inositol 1,4,5-trisphosphate; IP_3R, IP_3 receptor; PDE, phosphodiesterase; PGE_1, prostaglandin E_1; PKA, protein kinase A; PTH, parathyroid hormone; QPCR, quantitative PCR; RpcAMPS, adenosine 3′,5′-cyclic phosphorothioate-Rp; SERCA, SR/ER Ca^{2+}-ATPase; SQ 22536, 9-(tetrahydro-2′-furyl)adenine; SR, sarcoplasmic reticulum; WB, Western blot.

The online version of this paper contains supplemental material.

The Rockefeller University Press $30.00
J. Cell Biol. Vol. 183 No. 2 297–311
www.jcb.org/cgi/doi/10.1083/jcb.200803172

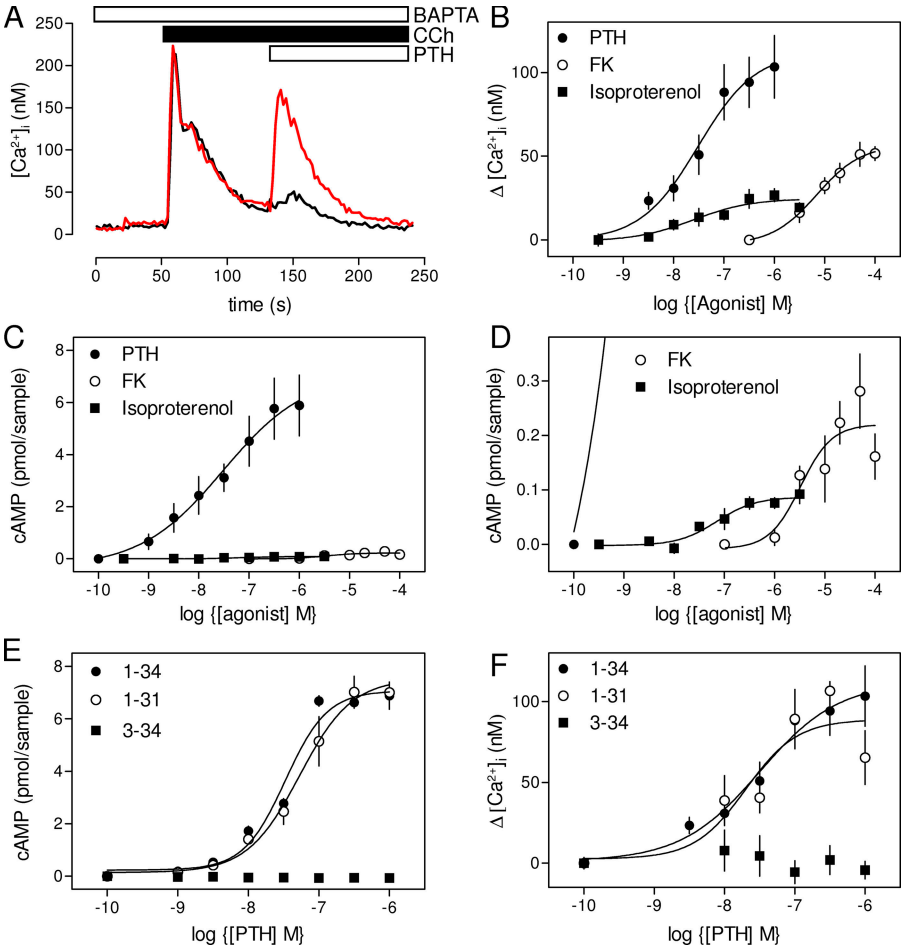

Figure 1. **Potentiation of CCh-stimulated Ca^{2+} release by stimuli that evoke cAMP formation.** (A) After addition of 10 mM 1,2-*bis*(*o*-aminophenoxy)ethane-*N*,*N*,*N*′,*N*′-tetraacetic acid (BAPTA) to chelate extracellular Ca^{2+}, 1 mM CCh stimulated transient release of Ca^{2+} from intracellular stores (black). 100 nM PTH in the continued presence of CCh then stimulated further Ca^{2+} release (red). (B) Effects of PTH, FK, and isoproterenol on the peak $[Ca^{2+}]_i$ in the continued presence of 1 mM CCh. (C and D) Stimulation of cAMP production by PTH, FK, and isoproterenol (D is an enlargement of C). (E and F) Stimulation of cAMP production (E) and potentiation of CCh-evoked Ca^{2+} signals (F) in response to PTH(1–34), PTH(1–31), and PTH(3–34). Others have shown that PTH(1–31) stimulates AC but not PKC, whereas PTH(3–34) stimulates PKC but not AC (Takasu et al., 1999). Results are means ± SEM from at least three experiments.

the related PTH receptors (types 1 and 2) belongs to the family of G protein–coupled receptors that includes those for secretin, calcitonin, and glucagon (Jüppner et al., 1991; Behar et al., 1996). PTH receptors share with these an ability to both stimulate adenylyl cyclase (AC) and increase cytosolic Ca^{2+} concentration ($[Ca^{2+}]_i$), but it is unclear how PTH stimulates Ca^{2+} release from intracellular stores. Some evidence suggests that PTH receptors stimulate PLC-β via Gq or Gi, and thus formation of IP_3 (Jüppner et al., 1991; Mahon et al., 2006). PTH receptors might also, like β-adrenoceptors, activate PLC-ε via cAMP (Schmidt et al., 2001). Other evidence suggests that Ca^{2+} release occurs without formation of IP_3 (Seuwen and Boddeke, 1995; Short and Taylor, 2000), and perhaps even in the presence of an antagonist of IP_3 receptors (IP_3R; Seuwen and Boddeke, 1995). We (Short and Taylor, 2000; Tovey et al., 2003) and others (Buckley et al., 2001) have suggested that PTH potentiates IP_3-evoked Ca^{2+} release, but the intracellular signals responsible have not been identified.

Here, we find that PTH, and other receptors that stimulate cAMP formation, communicate with IP_3R via intracellular "cAMP junctions," wherein cAMP passes directly from a specific isoform of AC (AC6) to a specific subtype of IP_3R (IP_3R2) to increase its IP_3 sensitivity. This identifies IP_3R as a new target for cAMP, an unexpected interaction between two ubiquitous signaling pathways, and a novel binary mode of cAMP signaling that allows robust digital recruitment of a response by graded concentrations of an extracellular stimulus.

Results

PTH potentiates IP_3-evoked Ca^{2+} release entirely via cAMP

Carbachol (CCh), via endogenous muscarinic receptors, stimulates PLC and thereby IP_3 formation and Ca^{2+} release from the intracellular stores of human embryonic kidney (HEK) cells (Fig. 1 A). In the absence of extracellular Ca^{2+}, stimulation of HEK cells stably expressing human type 1 PTH receptors (HEK-PR1 cells) with a supramaximal concentration of CCh caused an increase in $[Ca^{2+}]_i$ that returned to basal levels within 60–70 s. The addition of PTH, in the continued presence of CCh, evoked a further release of Ca^{2+} (Fig. 1 A). This additional Ca^{2+} release results from sensitization of IP_3R to IP_3 (Fig. S1, A and B, available at http://www.jcb.org/cgi/content/full/jcb.200803172/DC1; Short and Taylor, 2000; Tovey et al., 2003). Some analogues of PTH recruit other signaling pathways without stimulating AC (Takasu et al., 1999), but only the analogues that stimulate AC potentiated Ca^{2+} release (Fig. 1, E and F). Prostaglandin E_1 (PGE_1; unpublished data) and isoproterenol, which stimulate AC via their endogenous receptors, also potentiated CCh-evoked Ca^{2+} signals. So too did forskolin (FK), which directly stimulates AC (Fig. 1, B–D). However, 1,9-dideoxyforskolin (100 μM), an FK analogue that does not stimulate AC but mimics the AC-independent effects of FK (Zerr et al., 1996), had no effect on $[Ca^{2+}]_i$ either alone or with CCh (unpublished data). None of

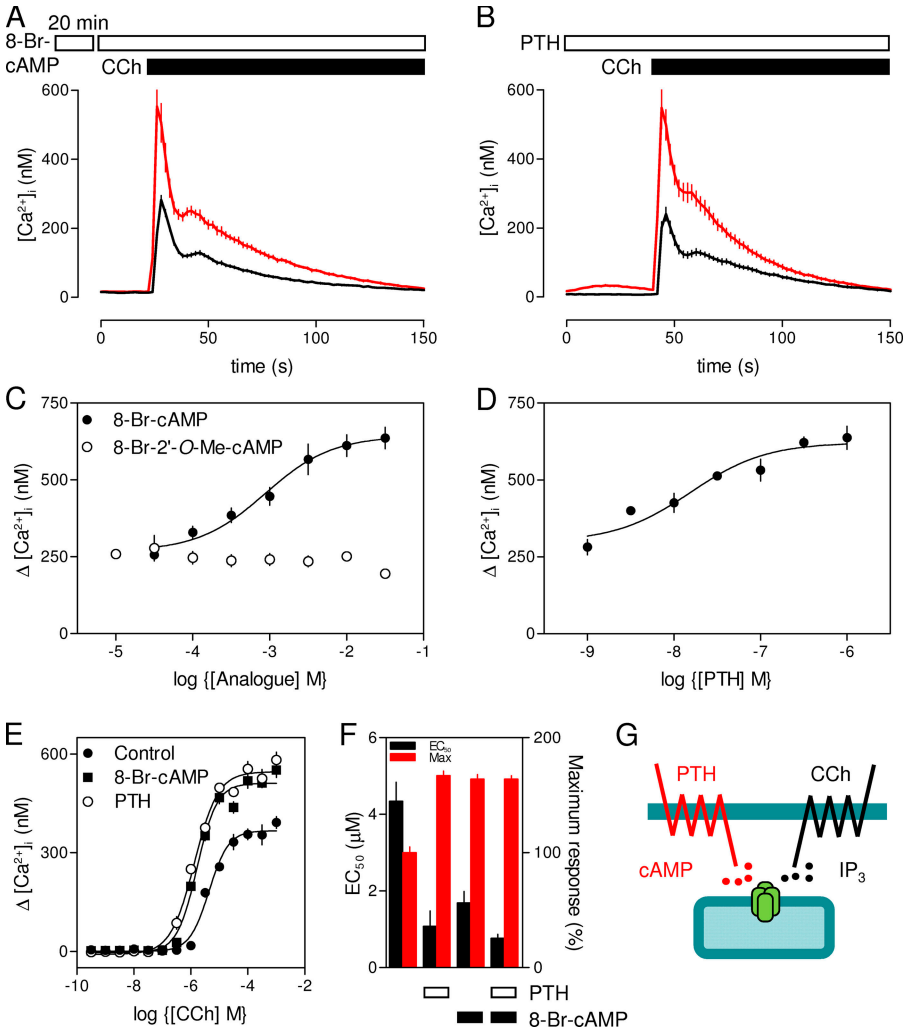

Figure 2. **Potentiation of CCh-stimulated Ca^{2+} release by 8-Br-cAMP.** (A and B) Ca^{2+} signals evoked by 1 mM CCh alone (black) or after prior treatment (red) with 8-Br-cAMP (A; 10 mM for 20 min) or PTH (B; 100 nM for 1 min). Results ($n > 3$ from one experiment; means ± SEM) are typical of more than six experiments. (C and D) Effects of 8-Br-cAMP, 8-Br-2′-O-Me-cAMP (C), and PTH (D) on peak $[Ca^{2+}]_i$ evoked by 1 mM CCh. (E) Effects of PTH (100 nM for 1 min) and 8-Br-cAMP (10 mM for 20 min) on CCh-evoked Ca^{2+} signals. (F) EC_{50} values and maximal responses (as a percentage of control) are shown for CCh-evoked Ca^{2+} signals after the indicated treatments. Results (C–F) are means ± SEM from at least three experiments. (G) cAMP entirely mediates potentiation of CCh-evoked Ca^{2+} release.

these stimuli significantly increased $[Ca^{2+}]_i$ in the absence of CCh (Fig. S1, C and D; Willoughby et al., 2006). Single cell analyses established that in most cells that responded to CCh (98 ± 1%), the Ca^{2+} signal was potentiated by PTH (99 ± 1%), isoproterenol (80 ± 4%), and FK (95 ± 3%).

PTH and a high concentration of the membrane-permeant analogue of cAMP, 8-Br-cAMP (30 mM), similarly potentiated CCh-evoked Ca^{2+} signals (Fig. 2, A–F); 8-Br-cGMP (30 mM) was ineffective (not depicted). Much lower (<100 μM) concentrations of 8-Br-cAMP activate PKA (He et al., 2003), but they did not significantly potentiate Ca^{2+} signals (Short and Taylor, 2000; Tovey et al., 2003). The low sensitivity to 8-Br-cAMP (half-maximal effective concentration, $EC_{50} = 0.87 \pm 0.37$ mM; Fig. 2 C) is important and is discussed further in later sections.

The extent to which the maximal Ca^{2+} release evoked by CCh can be enhanced is limited by the finite size of the intracellular Ca^{2+} stores, but there is no such limit on the extent to which the sensitivity to CCh can be increased. Two independently acting stimuli should cause an additive increase in CCh sensitivity. It is significant, therefore, that maximal concentrations of 8-Br-cAMP and PTH had the same effects on both the sensitivity of the Ca^{2+} signals to CCh and the maximal response (Fig. 2 E), and it is also significant that their effects were not additive (Fig. 2 F).

The nonadditive effects of PTH and 8-Br-cAMP on the EC_{50} for CCh-evoked Ca^{2+} signals establish the fact that cAMP is the only signal linking PTH receptors to sensitization of IP_3R (Fig. 2 G). G protein βγ subunits have been reported to stimulate IP_3R directly and so to cause release of Ca^{2+} (Zeng et al., 2003). PTH cannot work via this pathway because PTH does not alone cause Ca^{2+} release (Fig. S1), nor does somatostatin (1 μM), which activates Gi and thereby the release of βγ subunits (unpublished data; Law et al., 1993; Willoughby et al., 2007). We conclude that cAMP alone mediates the effects of PTH on IP_3R (Fig. 2 G). We provide additional evidence to support this key conclusion later (see Fig. 6).

cAMP sensitizes IP_3R independent of PKA and exchange proteins activated by cAMP (epacs)

All three subtypes of IP_3R can be phosphorylated by PKA, although at different sites and with different consequences (Bruce et al., 2003; Soulsby and Wojcikiewicz, 2007). IP_3R2 is the major (46%) IP_3R subtype in HEK cells (Table I), and in other cells expressing mainly IP_3R2, PKA potentiates IP_3-evoked Ca^{2+} release (Burgess et al., 1991; Bruce et al., 2003). In HEK-PR1 cells, PTH caused modest phosphorylation of IP_3R (Figs. 3 A

Table I. **Expression of subtypes of AC and IP_3R in HEK-PR1 cells**

Subtype	Percentage
AC1	12 ± 3
AC2	0
AC3	56 ± 7
AC4	0
AC5	0
AC6	5 ± 1
AC7	17 ± 3
AC8	0
AC9	10 ± 3
IP_3R1	19 ± 1
IP_3R2	46 ± 3
IP_3R3	35 ± 1

QPCR was used to measure relative levels (percentage of total) of mRNA encoding isoforms of AC and IP_3R in HEK-PR1 cells. Results are means ± SEM from three experiments, each performed in duplicate. The absence of AC2, AC4, and AC8 is consistent with a previous semiquantitative RT-PCR analysis, although a low level of AC5 was detected (Ludwig and Seuwen, 2002). The preponderance of IP_3R2 and IP_3R3 in HEK cells is consistent with results from immunoblotting (Wojcikiewicz, 1995).

and S2 B, available at http://www.jcb.org/cgi/content/full/jcb.200803172/DC1), and PKA very slightly (though not to a statistically significant degree) increased the sensitivity of the intracellular Ca^{2+} stores to IP_3 (see Fig. 4 A).

PTH, FK, and 8-Br-cAMP stimulated phosphorylation of many proteins in HEK-PR1 cells, and H89, an inhibitor of PKA, prevented this (Fig. 3 B, and see Fig. 5 F). But neither H89 (Fig. 3, C and E) nor other inhibitors of PKA (Figs. 3 F and S2, C–F) affected potentiation of the CCh-evoked Ca^{2+} signals. A kinase–anchoring proteins (AKAPs) contribute to PKA-mediated inhibition of IP_3R3 by cholecystokinin (Straub et al., 2002) and to many other PKA-mediated events (Wong and Scott, 2004). A membrane-permeant form of ht31 peptide (st-ht31), which uncouples AKAPs from PKA (Willoughby et al., 2006), blocked phosphorylation of many of the proteins phosphorylated in response to PTH and FK without affecting the response to 8-Br-cAMP (Fig. 3 B). But st-ht31 had no effect on the potentiation of CCh-evoked Ca^{2+} signals by FK (not depicted) or PTH (Fig. 3 D). We conclude that phosphorylation of IP_3R by PKA slightly potentiates responses to IP_3, and PTH stimulates modest phosphorylation of IP_3R, but the phosphorylation is not required for PTH to potentiate IP_3-evoked Ca^{2+} release.

Other proteins are also regulated by cAMP (Dremier et al., 2003), notably cyclic nucleotide-gated cation channels (CNGC; Rich et al., 2000) and epacs (Bos, 2003). Indeed, a cAMP-evoked increase in $[Ca^{2+}]_i$ has been proposed to result from activation of epac, Rap 2, and PLC-ε (Schmidt et al., 2001). By Western blotting (WB), we detected expression of epac-1 (but not epac-2) in HEK-PR1 cells (unpublished data), but no significant effect of isoproterenol, PTH, or FK alone on $[Ca^{2+}]_i$ (Fig. S1; Willoughby et al., 2006), although each potentiated responses to CCh (Figs. 1 B and S1). Nor did we detect formation of IP_3 in response to PTH (Short and Taylor, 2000). Epacs are less sensitive than PKA to cAMP (Bos, 2003), but 8-Br-2′-*O*-methyladenosine-3′,5′-cAMP selectively activates epacs (Christensen et al., 2003). Even very high concentrations (30 mM) of this analogue, which is more membrane-permeant than 8-Br-cAMP, had no effect on CCh-evoked Ca^{2+} signals, whereas 8-Br-cAMP potentiated them (Fig. 2 C). These results establish that potentiation of Ca^{2+} release by PTH results from sensitization of IP_3R rather than production of IP_3, and neither PKA nor epac is required.

In permeabilized HEK cells, high concentrations of cAMP (EC_{50} = 2.7 ± 1.0 mM; Fig. 4, A and B) increased the sensitivity of IP_3-evoked Ca^{2+} release by ∼4.5-fold. This is much greater than the ∼30% increase evoked by PKA (Fig. 4 A) but similar to the three- to fourfold increase in the sensitivity to CCh evoked by PTH or 8-Br-cAMP in intact cells (Fig. 2 E). The responses of permeabilized cells to cAMP and of intact cells to 8-Br-cAMP were unaffected by inhibition of PKA (by 10 μM H89; unpublished data). Potentiation of IP_3-evoked Ca^{2+} release by cAMP was mimicked by 8-Br-cAMP (EC_{50} = 324 ± 45 μM; Fig. 4, C and D) but not by 5′-AMP, ATP, ADP, or GTP (10 mM; not depicted). This low-affinity interaction between cAMP and IP_3R is consistent with only high concentrations of 8-Br-cAMP mimicking PTH in intact cells. Indeed, the sensitivities of intact (Fig. 2 C) and permeabilized cells (Fig. 4 D) to 8-Br-cAMP are similar. We conclude that cAMP binds directly to a low-affinity site on the IP_3R (or an associated protein) to increase its sensitivity to IP_3. The interaction is not mediated via changes in IP_3 binding because cAMP has no effect on ^{3}H-IP_3 binding to IP_3R2 (unpublished data). The affinity of this site for cAMP is ∼600-times lower than that of epacs (Bos, 2003) and ∼20,000-times lower than that of PKA or CNGC (Wong and Scott, 2004). It is unsurprising, therefore, that there is no known consensus sequence for cAMP binding within IP_3R (Dremier et al., 2003). A novel low-affinity site mediates the effects of cAMP on IP_3R.

Regulation of IP_3R by hyperactive cAMP junctions

Despite the evidence that cAMP entirely mediates sensitization of IP_3R (Figs. 1–4, S1, and S2), there is a massive disparity in the relationship between cAMP and Ca^{2+} for different stimuli (Fig. 5, A and B). This is most clear from the comparison of the amount of cAMP produced when each agonist causes $[Ca^{2+}]_i$ to increase by 30 nM (Fig. 5 C). The disparity is inconsistent with global cAMP signals serving as a universal currency, which are used similarly by each stimulus to regulate IP_3R. We note also that although HEK-PR1 cells express similar numbers of PTH receptors and β-adrenoceptors (see Fig. 7 E), maximal activation with PTH causes a much greater stimulation of AC (Fig. 1, C and D), which suggests that an active PTH receptor stimulates AC more effectively than does an active β-adrenoceptor.

Manipulation of cAMP levels by inhibiting either cAMP formation or its degradation by cyclic nucleotide phosphodiesterases (PDE) further highlights the inconsistent relationship between cAMP and potentiation of Ca^{2+} signals. 3-isobutyl-1-methylxanthine (IBMX), which inhibits most isoforms of PDE that degrade cAMP (Fisher et al., 1998), failed to enhance Ca^{2+} signals. Instead, it caused a slight inhibition (Fig. 5 E and S3 B, available at http://www.jcb.org/cgi/content/full/jcb.200803172/DC1) that became more pronounced with prolonged incubation (Short and Taylor, 2000). This probably

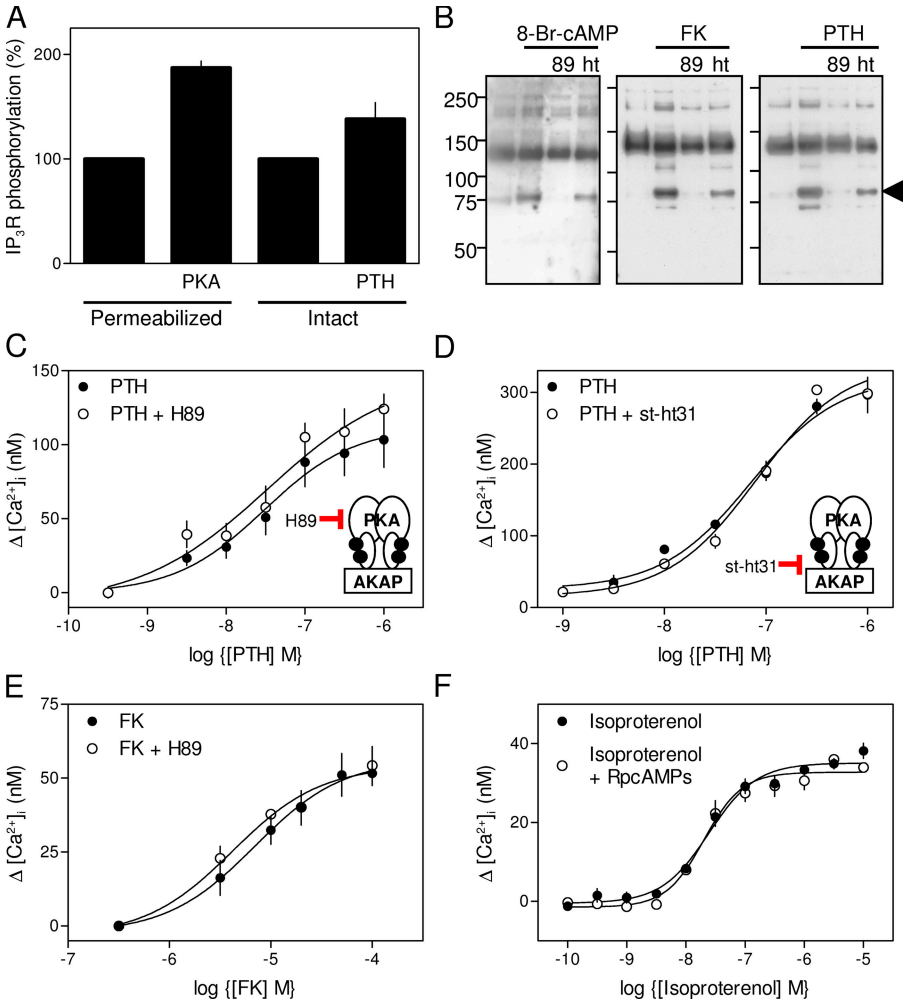

Figure 3. **PKA is not required for potentiation of CCh-evoked Ca^{2+} mobilization.** (A) IP_3R phosphorylation (AbP/AbIP_3R3) is expressed relative to levels detected in unstimulated cells (means ± SEM, n = 3–4). AbP is an anti-phospho Ser/Thr antibody (Table S1, available at http://www.jcb.org/cgi/content/full/jcb.200803172/DC1). (B) The effects of 8-Br-cAMP (10 mM for 20 min), FK (100 µM for 30 s), and PTH (100 nM for 30 s) on protein phosphorylation (assessed using AbP) alone or in the presence of H89 (89; 10 µM for 20 min) or st-ht31 (ht; 100 µM for 30 min). The arrow indicates the band used for quantification of protein phosphorylation in Fig. 5 F. M_r markers (kD) are indicated on the left. (C and D) The effect of H89 (C; 10 µM for 20 min) and st-ht31 (D; 100 µM for 30 min) on the ability of PTH to potentiate CCh-evoked Ca^{2+} mobilization. The targets of the inhibitors are shown in the insets. (E) The effect of H89 (10 µM for 20 min) on the ability of FK to potentiate CCh-evoked Ca^{2+} mobilization. (F) The effect of Rp-cAMPS (50 µM for 20 min) on the ability of isoproterenol to potentiate CCh-evoked Ca^{2+} signals. RpcAMPS was used to inhibit PKA because H89 decreased the sensitivity to isoproterenol by competing with it for occupancy of β-adrenoceptors (Fig. S2 E; Penn et al., 1999). Results (C–F) are means ± SEM, $n \geq 3$.

results from activation of PKA and loss of Ca^{2+} from intracellular stores via IP_3R made more sensitive to basal levels of IP_3 after their phosphorylation by PKA (Short and Taylor, 2000). More strikingly, massive inhibition of cAMP formation with a combination of inhibitors of AC (9-(tetrahydro-29-furyl)adenine [SQ 22536] and 2′,5′-dideoxyadenosine [DDA], referred to

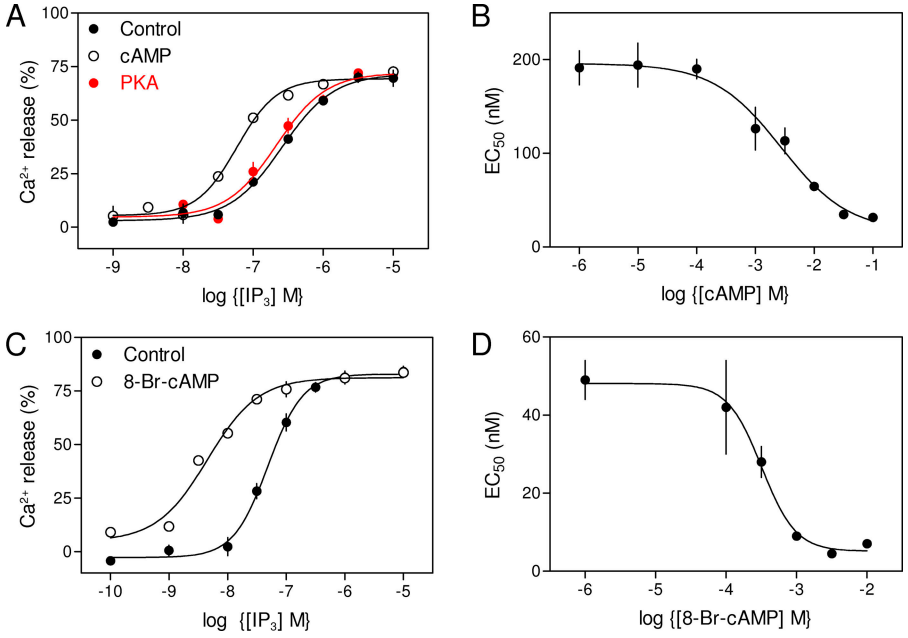

Figure 4. **Potentiation of IP_3-evoked Ca^{2+} release by cAMP in permeabilized cells.** (A) Ca^{2+} release from permeabilized HEK-PR1 cells evoked by IP_3 alone, after treatment with the catalytic subunit of PKA (100 units per milliliter for 10 min) or 30 mM cAMP. Results are shown as a percentage of the ionomycin-releasable Ca^{2+} store. (B) Concentration-dependent effect of cAMP on the EC_{50} for IP_3-evoked Ca^{2+} release from permeabilized HEK-PR1 cells. (C) Concentration-dependent stimulation of Ca^{2+} release by IP_3 alone and with 3 mM 8-Br-cAMP. (D) Concentration-dependent effect of 8-Br-cAMP on the EC_{50} for IP_3-evoked Ca^{2+} release. These results allow direct comparison with the effects of 8-Br-cAMP in intact cells (Fig. 2 C). The latter measurements were made after a 20-min preincubation with 8-Br-cAMP, and we have shown that although shorter preincubations cause lesser potentiation of Ca^{2+} signals, by 20 min, the response has reached its maximum. We conclude that 8-Br-cAMP equilibrates across the plasma membrane within 20 min. Results are means ± SEM, $n \geq 3$.

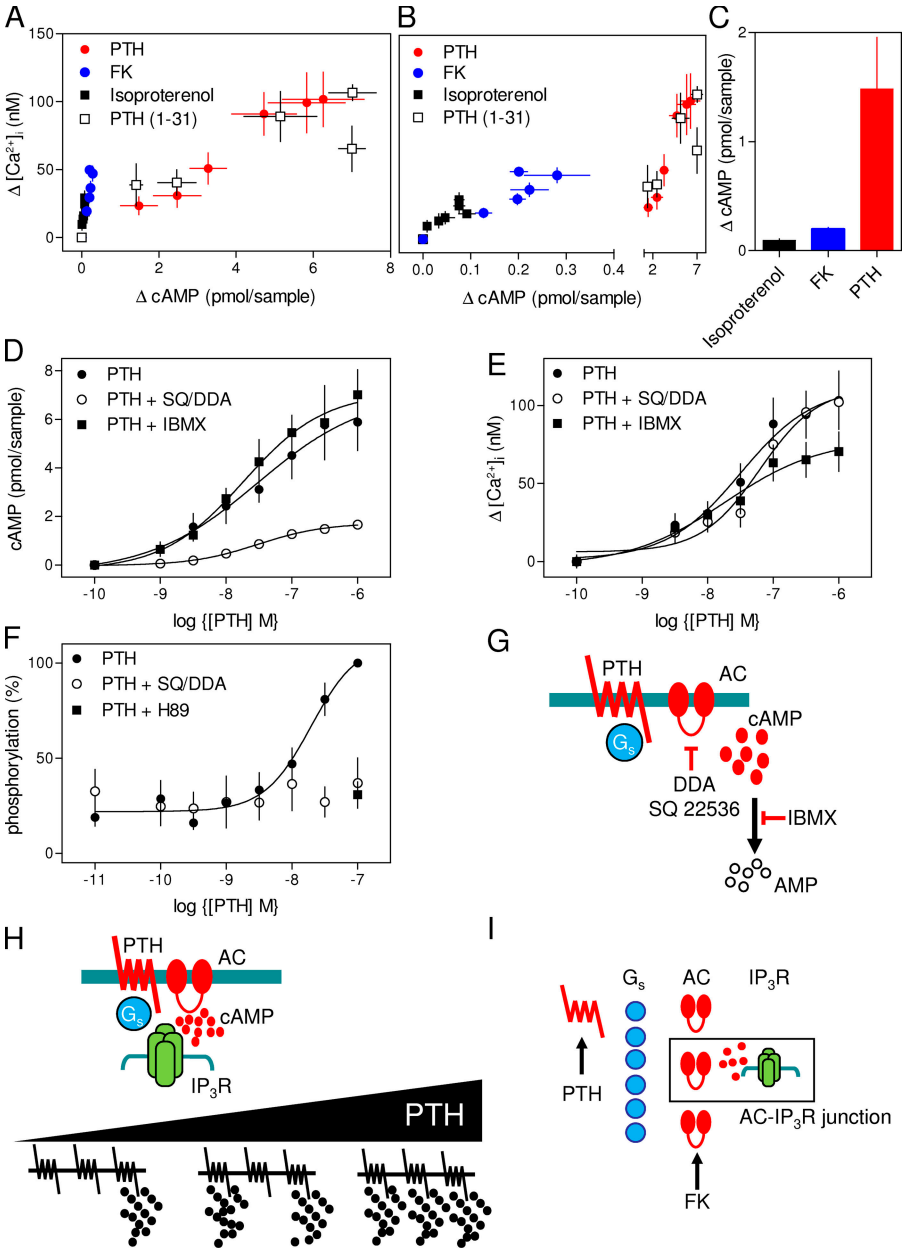

Figure 5. **Local cAMP signaling to IP_3R via hyperactive cAMP junctions.** (A–C) The relationship between the increase (Δ) in cAMP and $[Ca^{2+}]_i$ for each stimulus is shown (B is an enlargement of A to show FK and isoproterenol). The changes in cAMP associated with an increase in $[Ca^{2+}]_i$ of 30 nM evoked by each stimulus are shown in C. (D and E) The effects of inhibitors of AC (SQ/DDA: 1 mM SQ 22536; 200 μM DDA for 20 min) and PDE (IBMX: 1 mM for 20 min) on responses to PTH. Results are means ± SEM from four to five experiments. Similar results with FK and isoproterenol are shown in Fig. S3 (available at http://www.jcb.org/cgi/content/full/jcb.200803172/DC1). (F) Concentration-dependent phosphorylation of the 75-kD band (Fig. 3 B, arrow) after a 30-s treatment with PTH alone, and after pretreatment with SQ/DDA or H89 (means ± SEM, $n = 11$). (G) Targets of the inhibitors. (H) Sensitization of IP_3R in signaling complexes by receptors that generate supramaximal local concentrations of cAMP. The concentration-dependent effects of PTH (bottom) are proposed to arise from recruitment of these all-or-nothing junctions. (I) Steps preceding activation of AC might contribute to the surplus cAMP that allows communication between PTH and IP_3R to survive massive inhibition of AC, but for FK, only cAMP separates it from IP_3R. The AC–IP_3R interaction thus defines the minimal signaling complex, the "AC–IP_3R junction" (boxed).

hereafter as SQ/DDA; see the legend for Fig. 5) failed to attenuate the potentiated Ca^{2+} signals evoked by any concentration of FK, isoproterenol (Fig. S3, B and D), or PTH (Fig. 5 E). The latter was the case even though SQ/DDA abolished PTH-evoked protein phosphorylation (Fig. 5 F), and much lower concentrations of DDA blocked epac-mediated stimulation of PLC-ε (Schmidt et al., 2001).

Our results seem paradoxical. The effects of PTH on IP_3R are mediated entirely by cAMP (Fig. 1–4), yet in intact cells, there is no consistent relationship between cAMP and Ca^{2+} (Fig. 5, A–E).

Table II. **Effects of PTH, FK, and isoproterenol on cAMP and potentiation of CCh-evoked Ca^{2+} signals**

	Δ cAMP		Δ $[Ca^{2+}]_i$	
	Maximal response	EC_{50}	Maximal increase	EC_{50}
	fmol/sample		*nM*	
PTH	6,662 ± 1232	29 ± 7 nM	101 ± 14	31 ± 10 nM
FK	236 ± 29	3.3 ± 0.4 μM	55 ± 5	8.7 ± 2.0 μM
Isoproterenol	91 ± 15	113 ± 43 nM	30 ± 6	90 ± 24 nM

Results (means ± SEM, $n = 3$–10) show increases in cAMP and potentiation of the CCh-evoked Ca^{2+} signal evoked by each stimulus, with each response measured under identical conditions after a 30-s stimulation.

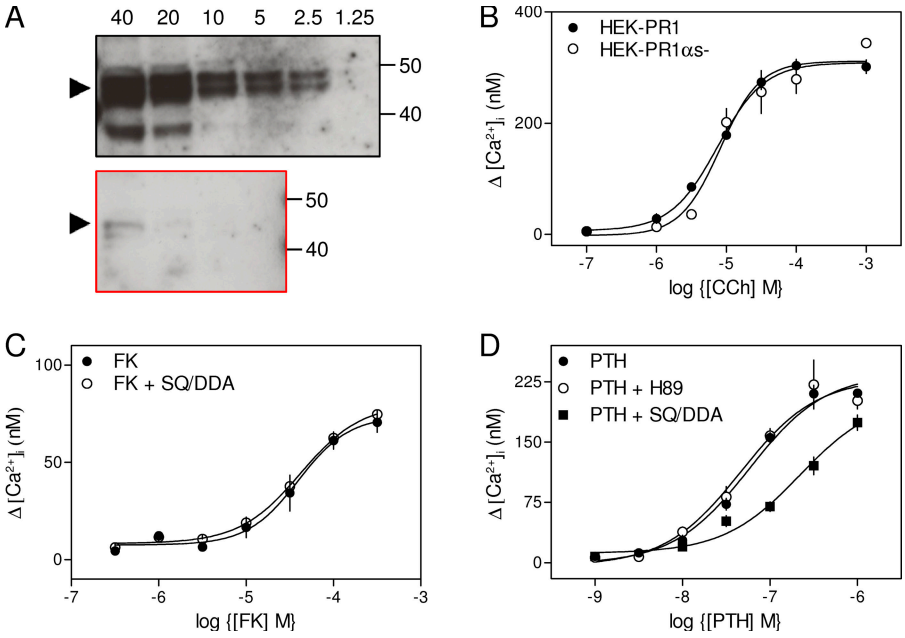

Figure 6. **Inhibition of Gαs expression confirms that cAMP mediates the effects of PTH on Ca^{2+} signals.** (A) WB showing expression of Gαs in HEK-PR1 cells before (black) and after (red) stable transfection with short hairpin RNA to Gαs (protein loadings are indicated in μg). Results are typical of at least three similar blots. Molecular weight markers are indicated in kD. (B) Effects of CCh on peak Ca^{2+} signals in the two cell lines. (C) Potentiation of CCh-evoked Ca^{2+} signals by FK alone or with SQ/DDA in HEK-PRαs$^-$ cells. (D) Potentiation of CCh-evoked Ca^{2+} signals by PTH alone or with SQ/DDA or H89 HEK-PRαs$^-$ cells. Results (B–D) are means ± SEM, n = 3–6.

This first led us to think that the effect of PTH on Ca^{2+} signals was not mediated by cAMP (Short and Taylor, 2000), but that conclusion is now untenable. Maximally activated receptors often generate more intracellular messenger than needed to evoke a maximal response. This allows downstream events to be more sensitive (lower EC_{50}) than earlier ones to the initial signal (Strickland and Loeb, 1981). Such systems are said to have "spare receptors" because activation of only a fraction of the receptors can evoke a maximal response. Responses to maximal stimulation may then survive even substantial inhibition of downstream signaling. But in our experiments, the EC_{50} values for cAMP formation and potentiation of Ca^{2+} signals, measured under identical conditions, are similar for each stimulus (Table II). Furthermore, even when maximal stimulation generates surplus signal, a globally distributed messenger cannot have a safety margin when it evokes a submaximal response: reducing the amount of messenger must reduce the response. Yet in our experiments, the Ca^{2+} signals evoked by every concentration of each stimulus were entirely insensitive to substantial inhibition of AC (Figs. 5 E and S3, B and D). How can cAMP mediate graded regulation of IP_3R and yet operate with a substantial safety margin at every level of stimulus intensity?

We suggest that cAMP sensitizes IP_3R independent of PKA and epac (Figs. 3 and S2). Signaling by cAMP must be local, and within a signaling complex, a receptor must generate substantially more cAMP than needed maximally to sensitize associated IP_3R (Fig. 5 H). Each complex, or cAMP junction, operates with a large safety margin so that even substantial inhibition of AC fails to compromise communication with IP_3R. The concentration-dependent effects of PTH (or FK) come from recruitment of increasing numbers of these hyperactive junctions and not from increased activity within each (Fig. 5 H). For receptors, the safety margin might arise at various steps of the signaling pathway: a single receptor might, for example, sustain the activity of more Gs than needed to stimulate sufficient AC to cause maximal activation of associated IP_3R (Fig. 5 I). But for FK, only cAMP lies between it and the IP_3R, and yet the Ca^{2+} signals evoked by any concentration of FK are also insensitive to substantial inhibition of AC (Fig. S3, A and B). Activation of a single AC can, therefore, deliver more cAMP than needed maximally to sensitize the IP_3R associated with it. This defines the minimal signaling complex: an AC–IP_3R junction (Fig. 5 I, box). The key point is that each active receptor (or AC) saturates the local signaling machinery and so functions as a local on–off switch. The very low affinity of the cAMP-binding site of the IP_3R (Fig. 4 B) effectively insulates each signaling complex from its neighbors because diffusion will reduce the cAMP concentration to below that needed to sensitize IP_3R within just a few nanometers of the complex (Rich et al., 2000). This digital signaling to IP_3R imposes no requirement for individual PTH receptors (or AC) to differ in their sensitivities; PTH binding to a uniform population of PTH receptors, governed by the law of mass action, is sufficient to generate a graded increase in the number of active receptors as the PTH concentration increases.

Our scheme (Fig. 5, H and I) predicts that AC and IP_3R are intimately associated, and that complete inhibition of cAMP formation within some junctions should more effectively attenuate Ca^{2+} signaling than partial inhibition of all junctions. Subsequent experiments confirm these predictions, but first we provide additional evidence that cAMP mediates the effects of PTH.

We established stable HEK-PR1 cell lines in which expression of Gαs was reduced by >95% by means of siRNA (Fig. 6 A). In these cells, CCh-evoked Ca^{2+} signals were normal (Fig. 6 B), FK potentiated them, and the response to FK was unaffected by inhibitors of AC (Fig. 6 C). However, whereas inhibition of PKA again had no effect on the Ca^{2+} signals evoked by PTH, the sensitivity to PTH was reduced by inhibition of AC in cells with reduced expression of Gαs (Fig. 6 D). These results show that when the safety margin for signaling between PTH receptors and IP_3R is eroded by removal of Gαs, the requirement for AC activity is unmasked. This further confirms that cAMP mediates the effects of PTH on IP_3R (Fig. 2 G).

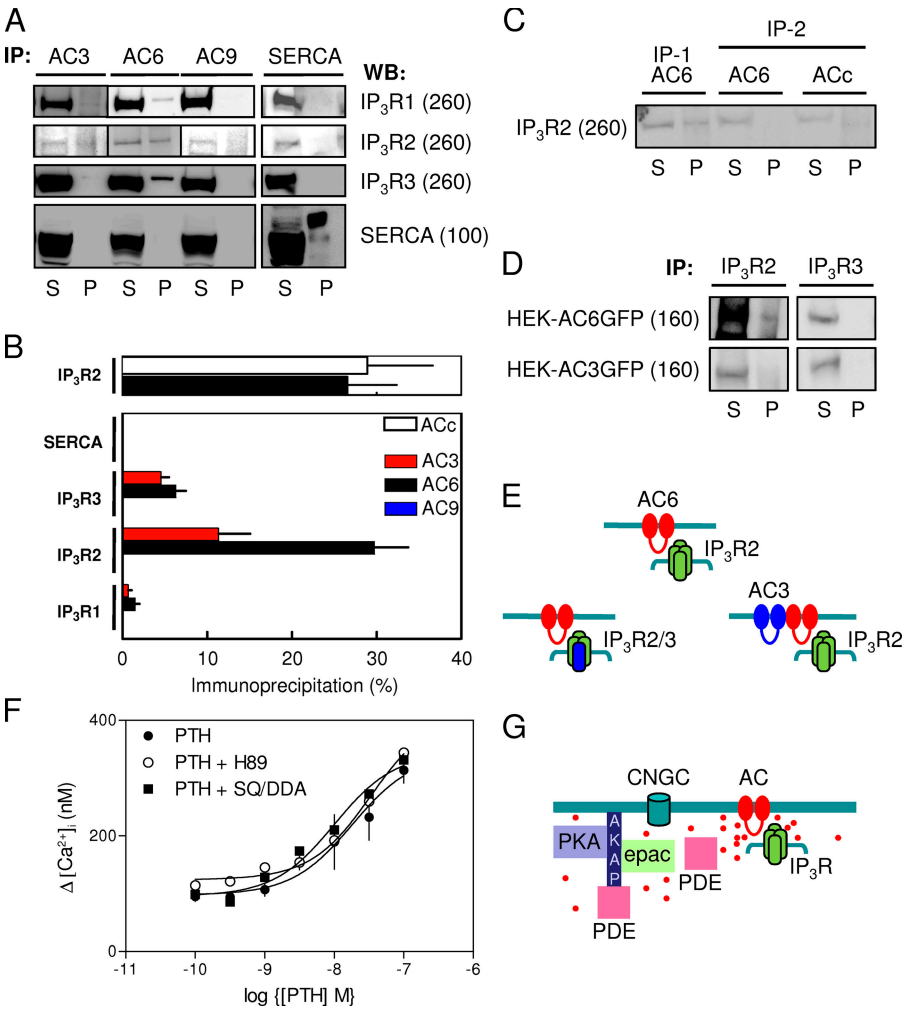

Figure 7. **AC6 and IP_3R2 are specifically associated.** (A) Typical results showing WB (P, pellet; S, supernatant) after IP of IP_3R or SERCA by the indicated antibodies. Here and in later panels, the calibrated molecular weights (kD) of the identified band are indicated. Black lines indicate that intervening lanes have been spliced out. (B) Percentages of total IP_3R1-3 detected in the pellet after IP with the indicated antibodies from HEK-PR1 cells (means ± SEM, $n \geq 3$). The efficiencies of the IP were similar for all $AbIP_3R$ (77 ± 3%, 74 ± 1%, and 78 ± 9% for IP_3R1-3, respectively). (C) After IP with AbAC6 (IP-1), a subsequent IP with AbAC6 or AbACc (IP-2) failed to precipitate IP_3R. Results typical of two independent experiments are shown. (D) Results typical of three experiments show WB with AbGFP after IP with $AbIP_3R2$ or $AbIP_3R3$ from HEK-PR1 cells transiently transfected with AC6-GFP or AC3-GFP (Fig. S4, available at http://www.jcb.org/cgi/content/full/jcb.200803172/DC1). The results show that only AC6 is immunoprecipitated, and only by $AbIP_3R2$. The results were not further quantified because overexpression of AC probably prevents more than a small fraction of it from associating with IP_3R. (E) We suggest that only IP_3R2 and AC6 interact directly (top), but hetero-oligomeric assemblies of AC or IP_3R may allow lesser amounts of IP_3R3 subunits or AC3 to associate with the AC6-IP_3R2 junction. (F) HEK-PR1 cells were stimulated with 100 nM PTH for either 30 s (as before; not depicted, but responses were indistinguishable from those after 5 min) or 5 min before addition of 30 µM CCh. Potentiation of the CCh-evoked Ca^{2+} signals by the indicated concentrations of PTH (5 min) alone or with SQ/DDA or H89 (20 min) are shown. The results (means ± SEM, $n \geq 3$) demonstrate that after prolonged treatment with PTH (to allow PKA-mediated recruitment of PDE), responses remain insensitive to inhibition of AC or PKA. (G) The association of AC6 and IP_3R2 is intimate enough to deny cAMP access to PDE as it passes between them, whereas local signaling between AC and the higher-affinity cAMP sensors (PKA, epac, or CNGC) occurs over longer distances and remains accessible to PDE. Diffusion of cAMP is sufficient to terminate signaling to IP_3R, whereas PDE assembled into signaling complexes regulates local events mediated by the other cAMP sensors.

AC6 and IP_3R2 are specifically associated

We used immunoprecipitation (IP) to determine whether any of the many isoforms of AC and IP_3R expressed in HEK cells are specifically associated. AC6 accounts for only 5% of the AC expressed in HEK cells (Table I), but an antibody to it (AbAC6) selectively precipitated 30% of IP_3R2 and lesser amounts of IP_3R3 and IP_3R1 (Fig. 7, A and B). An antibody that recognizes all mammalian AC isoforms (AbACc) selectively precipitated the same amount of IP_3R2 as AbAC6 (Fig. 7 B); and after IP with AbAC6, AbACc was unable to precipitate further IP_3R2 (Fig. 7 C). AC3 comprises 56% of the AC expressed in HEK cells (Table I), and an antibody to it (AbAC3) selectively precipitated some IP_3R2, but much less effectively than AbAC6 (Fig. 7, A and B). AC9 is also relatively abundant (10%), but IP_3R were not precipitated by AbAC9 (Fig. 7 B and S4 D, available at http://www.jcb.org/cgi/content/full/jcb.200803172/DC1). None of the AbAC precipitated the sarcoplasmic reticulum (SR)/ER Ca^{2+}-ATPase (SERCA), and nor were IP_3R precipitated by AbSERCA (Fig. 7, A and B). These results establish that the association of IP_3R with AC depends entirely on AC6. The lesser association of IP_3R with AC3 (Fig. 7 B) may result from hetero-oligomerization of AC3 with AC6. Both isoforms appear to dimerize (Fig. S4 B), and AC does form heterodimers (Willoughby and Cooper, 2007; Baragli et al., 2008). We considered whether PTH might itself regulate association of AC6 with IP_3R2, but the ability of AbAC6 to cause IP of IP_3R2 was unaffected by PTH (unpublished data).

Reciprocal IP from native cells using $AbIP_3R$ was impossible because available AC antibodies do not reliably detect endogenous AC in WB (Willoughby and Cooper, 2007). We therefore transiently expressed tagged human AC3 and AC6 in HEK cells, and confirmed that each AbAC selectively precipitated only the appropriate AC (Fig. S4, A–C). In the transiently transfected cells, $AbIP_3R2$ but not $AbIP_3R3$ selectively precipitated AC6, but not AC3 (Fig. 7 D). We conclude that AC6 and IP_3R2 are specifically associated. The lesser associations with AC3 and IP_3R3 probably result from interactions between heterotetrameric IP_3R (Fig. S2 A) and dimeric AC (Fig. S4 B) that include the essential IP_3R2 and AC6 subunits (Fig. 7 E).

Our analysis of AC and IP_3R expression (Table I and Fig. 8) suggest that a HEK cell expresses ~1,500 AC6 and ~13,300

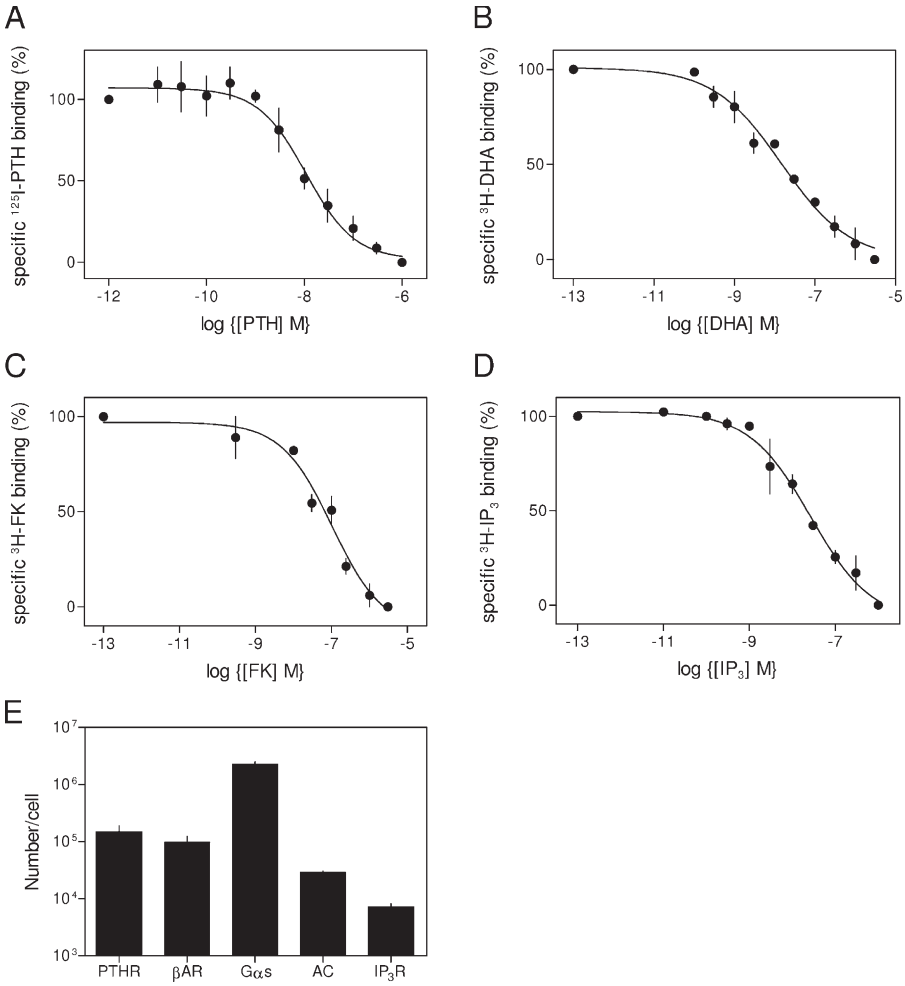

Figure 8. **Quantification of signaling proteins.** (A–D) Equilibrium competition binding curves for each of the ligands are shown. Results show the expression levels of PTH receptors (A), β-adrenoceptors (B), AC (C), and IP_3R (D) in HEK-PR1 cells. (E) Summary of the numbers of the signaling proteins expressed in each HEK-PR1 cell. For Gαs, this was calculated from calibrated WB, and for receptors and FK, it was computed from the K_d and the specific binding (S) determined for a defined concentration ([L]) of radioligand of known specific activity with the formula: $B_{max} = S(1+[L]/K_d)$. Means ± SEM, $n \geq 3$.

IP_3R2 subunits (~3,300 homotetrameric IP_3R2), and at least 30% of IP_3R2 (~1,000 IP_3R) are associated with AC6 (Fig. 7 B). These estimates cannot reliably define the stoichiometry of the IP_3R2–AC6 complex, but they are consistent with each AC6 associating with a single tetrameric IP_3R2 (Fig. 7 E).

AC–IP_3R junctions are inaccessible to PDE

In HEK cells, phosphorylation by PKA of PDE4D anchored to the plasma membrane by an AKAP (Willoughby et al., 2006) or recruited by arrestin (Willoughby et al., 2007) massively accelerates cAMP degradation. This rapidly attenuates the increase in cAMP immediately beneath the plasma membrane, whether evoked by PGE_1 (Willoughby et al., 2006) or isoproterenol (Willoughby et al., 2007). Our measurements (at 30 s) precede maximal activation of this PDE, which occurs ~1 min after stimulation with PGE_1 and ~3 min after stimulation of β_2-adrenoceptors (Willoughby et al., 2006). However, when the interval between PTH and CCh additions was extended to 5 min to allow maximal activation of anchored PDE4D by PKA, the potentiated Ca^{2+} signals remained insensitive to inhibition of AC or PKA at every concentration of PTH (Fig. 7 F). These results demonstrate that even when PDE is massively stimulated, inhibition of AC fails to attenuate cAMP-mediated communication with IP_3R. Nor is communication with IP_3R improved by inhibiting PDE either directly with IBMX (Figs. 5 E and S3, B and D) or indirectly by preventing its recruitment and activation by PKA-mediated phosphorylation (Fig. 3, A and B; and Figs. 7 F and S2). We conclude that the interaction between AC6 and IP_3R2 is more intimate than that between AC and PKA, epac, or CNGC (Willoughby et al., 2006), even though the latter detect only cAMP immediately beneath the plasma membrane. Only the IP_3R allows cAMP to evade PDE as it passes from AC to its target (Fig. 7 G). We conclude that AC6 and IP_3R2 are specifically associated, and their intimacy is sufficient to allow cAMP to pass between them without encountering PDE. This reveals an important distinction between two different modes of cAMP signaling: binary (to IP_3R) and analogue (to PKA and epac). Because epac and PKA bind cAMP with high affinity, they can respond in a graded fashion to cAMP diffusing to them from a distant AC, but they then assemble with PDE to ensure effective local degradation of the messenger (Dodge-Kafka et al., 2005; Willoughby et al., 2006, 2007). In contrast, IP_3R, with their low affinity for cAMP, must be very close to AC, but diffusion alone is enough to terminate the signaling. Both modes of cAMP signaling generate spatially organized responses: the analogue mode used by high-affinity cAMP sensors relies on local degradation of cAMP, whereas the binary mode requires local synthesis of cAMP to deliver it at high concentration to a low-affinity cAMP sensor (Fig. 7 G).

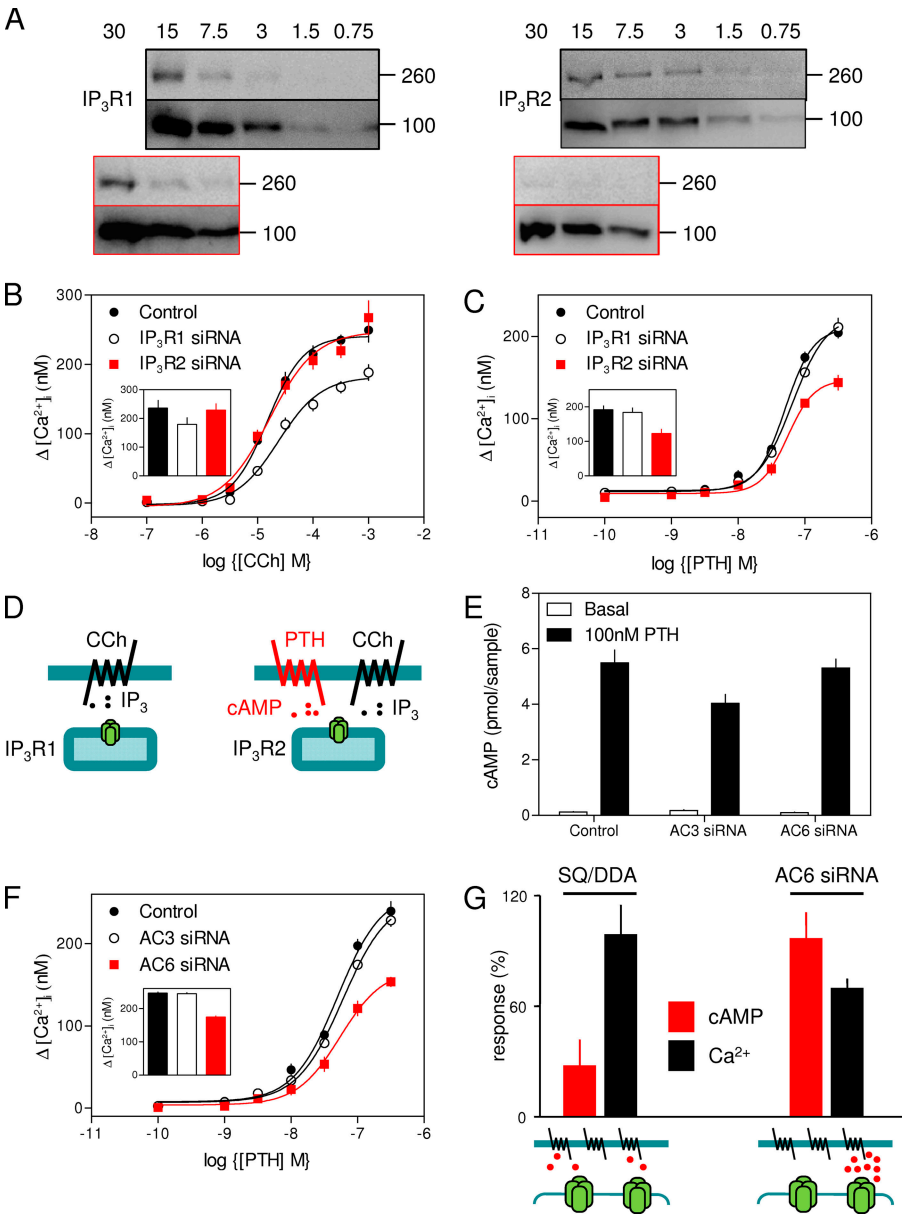

Figure 9. **IP_3R2 and AC6 are specifically required for PTH to potentiate IP_3-evoked Ca^{2+} release.** (A) WB (representative of five experiments) shows the effects of siRNA (boxed in red) on the expression of IP_3R1 (260 kD), IP_3R2 (260 kD), and β-adaptin (100 kD; protein loadings are given in μg; molecular weight standards are indicated in kD). Each block shows IP_3R above and β-adaptin below. (B and C) Effects of reducing IP_3R1 or IP_3R2 expression on CCh-evoked Ca^{2+} signals (B) and the potentiation of CCh (1 mM)-evoked Ca^{2+} signals by PTH (C). The latter were measured as in Fig. 1 A. Results are means ± SEM of triplicate determinations from a single experiment. Insets show the maximal responses (means ± SEM) from four to five independent siRNA treatments. (D) The Ca^{2+} release evoked by CCh alone requires IP_3R1, whereas the Ca^{2+} release evoked by CCh acting in concert with cAMP specifically requires IP_3R2. (E and F) Effects of reducing AC3 or AC6 expression on PTH-evoked cAMP formation (E) and on the potentiation of CCh-evoked Ca^{2+} signals by PTH (F). Results are means ± SEM from at least five independent siRNA treatments; the main panel in F shows means ± SEM of triplicate determinations from a single experiment. (G) Summary showing that uniform inhibition (by ∼60–70%) of AC by SQ/DDA massively inhibits PTH-evoked cAMP formation, whereas a comparable (∼60–70%) loss of AC6 (using siRNA) has no detectable effect on cAMP formation but attenuates PTH-mediated Ca^{2+} signaling. Results indicate means ± SEM, $n \geq 3$.

Potentiation of IP_3-evoked Ca^{2+} signals by PTH specifically requires AC6 and IP_3R2

We used siRNA to inhibit selectively the expression of IP_3R2, IP_3R1, AC3, and AC6 (Fig. 9 A and Table III). Although siRNA also reduced IP_3R3 expression, these cells failed to attach to the plates used for Ca^{2+} and cAMP assays, preventing further analysis. Loss of IP_3R1 decreased the Ca^{2+} signals evoked by CCh without affecting their potentiation by PTH. In contrast, loss of IP_3R2 had no affect on the Ca^{2+} signals evoked by CCh alone but attenuated their potentiation by PTH (Fig. 9, B and C). These results suggest that the muscarinic receptors that alone evoke Ca^{2+} release are distributed differently to those that release Ca^{2+} in synergy with cAMP. IP_3R1 mediates the Ca^{2+} release evoked by CCh alone, whereas IP_3R2 mediates the response to CCh with cAMP (Fig. 9 D). Loss of AC3, the major AC isoform, reduced PTH-evoked cAMP formation, though without affecting the ability of PTH to potentiate CCh-evoked Ca^{2+} signals. Conversely, loss of AC6 had no detectable effect on PTH-evoked cAMP formation but attenuated PTH-evoked Ca^{2+} signals (Fig. 9, E and F). The Ca^{2+} release evoked by CCh alone was unaffected by loss of AC3 or AC6 (Fig. S4, E and F). These results confirm that the specific association between IP_3R2 and AC6 revealed by IP (Fig. 7) underlies the ability of PTH to potentiate CCh-evoked Ca^{2+} signals.

Focal inhibition of AC more effectively inhibits Ca^{2+} signaling than global inhibition

Because we propose that each cAMP junction operates with a large safety margin (Fig. 5 H), complete inhibition of AC within some junctions should more effectively inhibit sensitization of IP_3R than partial inhibition of AC within all junctions. SQ 22536 and DDA are low-affinity inhibitors of all AC (Reid et al., 1990) that should rapidly and uniformly distribute their inhibition across all AC. Such uniform inhibition of AC by ∼70% does not

inhibit Ca^{2+} signaling (Fig. 5, D and E; and Fig. S3). In contrast, inhibition of AC6 expression by siRNA is expected to cause random loss of AC from individual signaling complexes, each perhaps comprising only a dimeric AC associated with a single IP_3R (Fig. 5, H and I). A 62% loss of AC6 (~3% of total AC) had no detectable effect on PTH-evoked cAMP formation but inhibited PTH-mediated Ca^{2+} signaling by 30% without affecting the sensitivity to PTH (EC_{50} = 63 ± 3 nM and 54 ± 5 nM, before and after loss of AC6, respectively; Fig. 9 F). These results confirm our second prediction. When all AC (and thus all AC6) is uniformly inhibited by 60–70% (by SQ/DDA), Ca^{2+} signaling is unaffected. In contrast, the same overall loss of AC6 activity, though distributed in an all-or-nothing fashion between junctions (by reducing AC6 expression), reduces the magnitude of the Ca^{2+} signals without affecting the PTH sensitivity of the remaining junctions (Fig. 9 G).

Direct cAMP-mediated signaling between AC and IP_3R

We can compare quantitatively the relationships between cAMP and Ca^{2+} because each was measured at the same time under identical conditions, all cells responded similarly, and cAMP alone mediates the effects of PTH (Fig. 1–4). The similar sensitivity of intact and permeabilized cells to 8-Br-cAMP (Figs. 2 C and 4 D) confirms the fact that permeabilized cells retain their sensitivity to cAMP. This allows comparisons of the cAMP sensitivity of IP_3R in permeabilized cells with the calculated concentrations of cAMP evoked by PTH if cAMP were uniformly distributed through the cytosol. For PTH, which produces more cAMP than other stimuli (Fig. 1, C and D), the calculated cAMP concentrations are ~1,000-fold too low to modulate IP_3R. The disparity is even greater when AC is inhibited and the AC–IP_3R junctions operate with a reduced safety margin. Therefore, the half-maximal Ca^{2+} signal evoked by PTH is associated with an estimated global cAMP concentration of ~500 nM (Fig. 10 A), whereas the half-maximal response in permeabilized cells requires a 5,400-fold higher concentration of cAMP (2.7 mM; Fig. 4 B).

Subplasma membrane microdomains of cAMP occur in many cells, including HEK cells (Rich et al., 2000; Willoughby et al., 2006, 2007). But the highest local concentrations of free cAMP achieved, whether measured or estimated from the activity of AC and cAMP diffusion (Rich et al., 2000), exceed the global cytosolic cAMP concentration by no more than 10-fold, even within a few nanometers of AC. Cytosolic cAMP concentrations, even very close to AC, are far too low to affect IP_3R directly, and restricting the escape of cAMP with internal membranes like the ER (Rich et al., 2000) might further increase the local cAMP concentration by no more than approximately twofold (Olveczky and Verkman, 1998). Cyclic AMP cannot reach IP_3R via the cytosol at concentrations sufficient to cause their sensitization to IP_3. We instead suggest that the intimate association between IP_3R2 and AC6 (Fig. 7) allows cAMP to pass directly from AC to IP_3R in a manner analogous to substrate channeling in enzyme complexes (Fig. 10 B; Huang et al., 2001).

Discussion

AC6 and IP_3R2: the most intimate mode of cAMP signaling

We have shown that receptors that stimulate cAMP formation sensitize IP_3R to IP_3 via a pathway that requires neither PKA nor epac, but which is instead mediated by a novel low-affinity cAMP-binding site on either the IP_3R itself or an associated protein. A complex of AC6 and IP_3R2 is uniquely required for PTH to potentiate IP_3-evoked Ca^{2+} release. Within each AC–IP_3R junction, cAMP is delivered directly to the associated IP_3R at a supersaturating concentration, allowing the junction to work as a robust on–off switch. Graded responses to changes in the intensity of the extracellular stimulus arise from digital recruitment of AC–IP_3R junctions and not from graded activity of individual junctions. The presence of AC6 in these junctions is significant because AC6 is inhibited by Ca^{2+} (Willoughby and Cooper, 2007). It is therefore likely that within the AC6–IP_3R2 junction, there will be a reciprocal interplay between AC6 and IP_3R, with AC6 potentiating IP_3R activity via cAMP, and active IP_3R inhibiting AC6 via Ca^{2+} (Fig. 10 B). These feedback interactions may generate highly localized oscillations in both Ca^{2+} and cAMP similar to those observed in whole cells (Gorbunova and Spitzer, 2002; Dyachok et al., 2006).

The AC–IP_3R junction suggests an analogy with excitation–contraction coupling in striated muscle, where voltage-sensing dihydropyridine receptors (DHPR) in the plasma membrane regulate opening of ryanodine receptors in the SR across a narrow (~10 nm) junctional complex (Fig. 10 D). Coupling of these proteins has evolved from chemical coupling mediated by Ca^{2+} (cardiac excitation–contraction coupling) to a physical coupling between the two apposed proteins (vertebrate skeletal muscle; Di Biase and Franzini-Armstrong, 2005). Junctional complexes similar to those in striated muscle occur also in nonexcitable cells;

Table III. **Selective inhibition of expression of AC and IP_3R isoforms**

siRNA	AC3	AC6	IP_3R1	IP_3R2	IP_3R3
AC3	40 ± 2[a]	123 ± 35	103 ± 9	93 ± 14	87 ± 7
AC6	101 ± 27	38 ± 8[a]	91 ± 6	101 ± 12	92 ± 10
IP_3R1	ND	ND	36 ± 6[a]	103 ± 9	138 ± 7
IP_3R2	ND	ND	96 ± 18	≤5[a]	77 ± 6

Quantification of levels of expression (percentage of control, means ± SEM from three to five independent transfections) of the isoforms of AC and IP_3R from HEK-PR1 cells treated with the indicated siRNA. Samples were taken from the same cells that were used for measurements of $[Ca^{2+}]_i$ and cAMP (Fig. 9). WB was used to quantify IP_3R expression and QPCR for AC (available antibodies are incapable of detecting endogenous levels of AC). ND, not determined.

[a]Indicates the extent to which expression of the target protein was reduced.

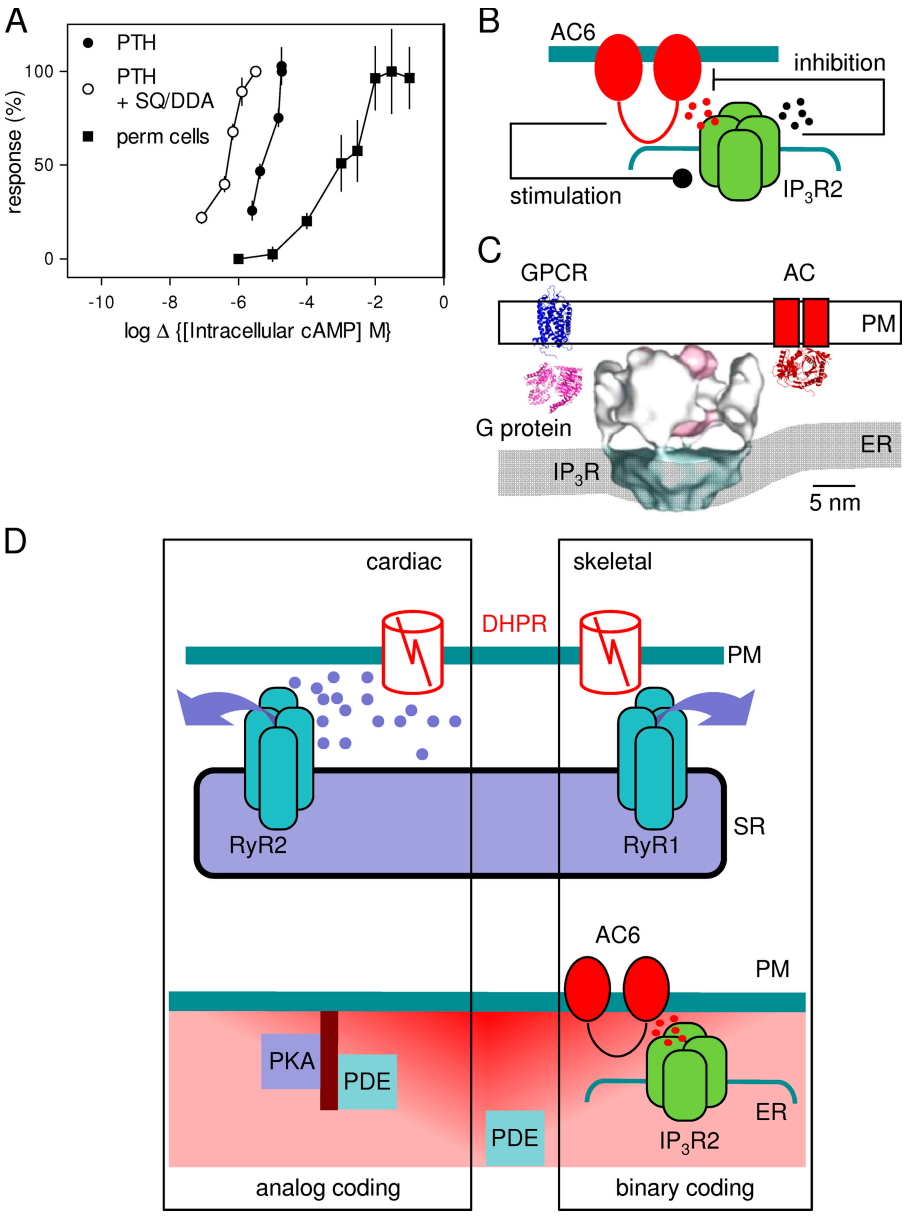

Figure 10. **Binary and analogue signaling by cAMP.** (A) Comparison of the effects of cAMP on IP_3-evoked Ca^{2+} release from permeabilized cells with estimates of the global cAMP concentration associated with agonist-mediated potentiation of Ca^{2+} signals in intact cells. A typical HEK cell has a radius of 8.4 µm and thus a total volume of ~2.5 pl (Rich et al., 2000). Each well used for cAMP assays contained a mean of 4.8×10^5 cells, and our results show cAMP levels determined in 20% of the sample taken from each well, equivalent therefore to 96,000 cells and a total cytosolic volume of 0.24 µl. Maximal stimulation with each agonist would generate a uniformly distributed cytosolic cAMP concentration of up to ~28 µM (PTH), ~1 µM (FK), and ~380 nM (isoproterenol). Means ± SEM, n = 3–6. (B) AC6 and IP_3R2 form an intimate junction that allows cAMP to pass directly to IP_3R2, enhancing its activity. Ca^{2+} released by the IP_3R may then locally inhibit AC6. The interplay may allow local oscillations in both cAMP and Ca^{2+} concentration. (C) AC, IP_3R, Gs, and a G-protein-coupled receptor (GPCR) are each drawn to approximate scale, with the ER and plasma membrane (PM) separated by 10–15 nm (Treves et al., 2004; Luik et al., 2006). (D) The IP_3R–AC junction allows a low-affinity cAMP-sensor (IP_3R2) to respond robustly to saturating concentrations of cAMP delivered directly to it by AC. Higher affinity cAMP sensors (e.g., PKA) can be more remote from AC and respond to local gradients of cAMP. Although the binary coding requires local delivery of cAMP, the analogue coding requires its local degradation. The two modes of cAMP signaling invite comparison with the evolution of excitation–contraction coupling in striated muscle, where coupling between the PM voltage-sensor (DHPR) and ryanodine receptor (RyR) in the SR of striated muscle probably evolved from chemical coupling mediated by Ca^{2+} (cardiac muscle) to conformational coupling (skeletal muscle; Di Biase and Franzini-Armstrong, 2005).

they are implicated in Ca^{2+} signaling (Treves et al., 2004; Varnai et al., 2007), and their width (10–15 nm) would allow IP_3R and AC to abut (Fig. 10 C). We speculate that the AC6–IP_3R2 complex may occur within such junctions, and that its evolution from the looser relationship between AC and PKA mediated by soluble cAMP may be similar to the evolution of conformational coupling in skeletal muscle from Ca^{2+}-mediated coupling in cardiac muscle (Di Biase and Franzini-Armstrong, 2005). The difference is that AC6–IP_3R2 communication requires not only direct contact but also passage of a constrained messenger, cAMP, between them (Fig. 10 B).

The IP_3R is a new and important target of cAMP. The AC6–IP_3R2 complex allows cAMP to pass directly to IP_3R and increase its sensitivity to IP_3. These cAMP junctions (Fig. 10 B) allow robust signaling to IP_3R because they are hyperactive on–off switches (Fig. 5 H). Increasing stimulus intensities recruit additional junctions, rather than increasing the activity within individual junctions. Signaling by cAMP to IP_3R is binary, requires direct contact between AC6 and IP_3R2, and relies on diffusion of cAMP to terminate the response of each junction. Other sensors with greater affinity for cAMP, like PKA and epac, respond to graded changes in local cAMP concentration (analogue signaling) and rely on PDE activity to shape local signaling events (Figs. 7 G and 10 D). These different modes of signaling considerably increase the versatility of cAMP as an intracellular messenger.

Materials and methods

Materials

DDA, cAMP, 8-Br-cAMP, 8-Br-cGMP, H89 dihydrochloride, ionomycin, KT5720, adenosine 3′,5′-cyclic phosphorothioate-Rp (RpcAMPS), SQ 22536, and 1,2-*bis*(*o*-aminophenoxy)ethane-*N*,*N*,*N*′,*N*′-tetraacetic acid (BAPTA) were obtained from EMD. 8-Br-2′-*O*-methyladenosine-3′,5′-cAMP was obtained from Biolog. IP_3 was obtained from American Radiolabeled Chemicals. Thapsigargin was obtained from Alomone Laboratories. Human PTH fragments were obtained from Bachem; unless specifically stated, "PTH" denotes human PTH(1–34). Cell culture media, G-418, Fluo-4AM, Fura-2AM, Mag-fluo-4AM, and Pluronic F-127 were obtained from Invitrogen.

Acetic anyhydride, CCh, carbonyl cyanide-*p*-trifluoromethoxyphenylhydrazone, FK, 1,9-dideoxyforskolin, IBMX, (±)-isoproterenol hydrochloride, the porcine catalytic subunit of PKA, and triethylamine were obtained from Sigma-Aldrich. St-ht31 was obtained from Promega.

Cells, vectors, and siRNA

HEK-PR1 cells were cultured as described previously (Short and Taylor, 2000). For siRNA-mediated inhibition of AC or IP_3R expression, HEK-PR1 cells were seeded into 6-well plates (2.5×10^5 cells per well). After 24 h, the medium was replaced (2.5 ml) and Stealth siRNA duplex (30 pmol; Invitrogen) was added in Opti-MEM 1 + Glutamax (0.5 ml) containing 1% lipofectamine RNAimax (Invitrogen). The siRNA sequences (5′–3′) were: IP_3R1 (GGCCUGAGAGUUACGUGGCAGAAAU), IP_3R2 (GAGAAGGCUCGAUGCUGAGACUUGA), AC3 (CCUCUGAAGAUGAGCACGAGCUCAA), and AC6 (CCAGCAUCUUCCUGCUGCUGCUAAU). After 24 h, cells were reseeded into 96-well (2,500 cells per well) or 6-well plates (10^5 cells per well), and after a further 48 h, the transfection with siRNA was repeated. Cells were incubated for a further 72 h before use. A modified pSUPER vector (Brummelkamp et al., 2002) was used to generate short hairpin RNA–mediated knockdown of Gαs in HEK-PR1 cells. Transfected cells were selected using 10 µg/ml blasticidin and 800 µg/ml G418, and clonally isolated cells were used to establish the seven cell lines used for analyses of cAMP and Ca^{2+} signaling.

Transient expression of tagged AC3 and AC6

The open reading frames for human AC3 (AK122926) in pME18SFL3 (National Institute of Technology and Evaluation Biological Resource Center) and AC6 (BC064923) in pCMV-Sport 6 (GeneService) were cloned as EcoRI—XhoI fragments into pENTR1a (Invitrogen). A Flag (AC3) or Myc (AC6) tag was introduced at the N terminal by PCR. Tagged and untagged AC constructs were subcloned into the pEGFP-C2 vector (Clontech Laboratories, Inc.) to generate AC constructs N-terminally tagged with EGFP (Fig. S4 A). HEK-PR1 cells were transfected using lipofectamine and used after 2 d.

Measurements of $[Ca^{2+}]_i$

Near confluent cultures of HEK-PR1 cells grown in 96-well plates and loaded with Fluo-4 were used for measurements of $[Ca^{2+}]_i$ in cell populations using a FlexStation 96-well fluorescence spectrometer (MDS Analytical Technologies; Tovey et al., 2006). The results reported herein span >4 yr, but all direct comparisons between stimuli or between cAMP and Ca^{2+} were made in parallel experiments. Single cell imaging of $[Ca^{2+}]_i$ was performed as described previously (Tovey et al., 2003), and after correction for autofluorescence, fluorescence ratios were calibrated to $[Ca^{2+}]$ using Ca^{2+} standard solutions (Invitrogen). CCh stimulation was always in Ca^{2+}-free Hepes-buffered saline (HBS; except in Fig. S1, C and D). A low-affinity luminal Ca^{2+} indicator was used to measure IP_3-evoked Ca^{2+} release from permeabilized cells (Tovey et al., 2006).

Measurements of cAMP

HEK-PR1 cells in 24-well plates were cultured for 2–3 d (as described in a preceding section). They were washed twice in HBS (135 mM NaCl, 5.9 mM KCl, 1.2 mM $MgCl_2$, 1.5 mM $CaCl_2$, 11.6 mM Hepes, and 11.5 mM glucose, pH 7.3) and then incubated under identical conditions (including addition of CCh) to those used for measurements of $[Ca^{2+}]_i$; the only difference was the omission of Fluo-4-AM and Pluronic F-127 from the 1-h incubation. After stimulation, the medium was aspirated, and the cells were lysed by the addition of acidified ice-cold ethanol (10 mM HCl in absolute ethanol). Dried extracts in 500 µl of medium (50 mM sodium acetate, 1 mM theophylline, and 1 mg/ml BSA, pH 5.0) were acetylated by rapid sequential addition of 10 µl triethylamine and 5 µl acetic anhydride. Acetylated cAMP content was determined by RIA using acetylated standards prepared from a cAMP stock calibrated by its UV absorption (ε_{258} = 14,100). For RIA (Brooker et al., 1979), rabbit antiserum to acetylated cAMP (P.D. Marley, University of Melbourne, Melbourne, Australia; Marley et al., 1991) was used at a final concentration of 1:9,000, and 8.4 TBq/mmol adenosine 3′,5′-cyclic phosphoric acid, 2′-*O*-succinyl[^{125}] iodotyrosine methyl ester (PerkinElmer) was used as tracer. Assays (300 µl) included 100 µl of sample. After incubation for 48 h at 4°C, 2 mg/ml BSA and 2 mg/ml Norit A charcoal were added in 50 mM sodium phosphate buffer at pH 7.4, and the free and antibody-bound tracer were separated (1,000 *g* for 10 min).

IP and Western blotting

All procedures were performed at 4°C. A confluent 175-cm^2 flask of HEK-PR1 cells was washed in 50 ml PBS supplemented with protease inhibitors (one tablet of Roche complete protease inhibitor per 50 ml). Cells were scraped into 1.5 ml solubilization medium, sonicated (three times for 10 s), and incubated with rotation for 1 h. Solubilization medium had the following composition: 140 mM NaCl, 5 mM NaF, 10 mM Tris, 1 mM $Na_4P_2O_7$, 0.4 mM Na_3VO_4, 1% Triton X-100, pH 7.4, and one mini-tablet of Roche protease cocktail inhibitor per 10 ml. Cell debris was removed by centrifugation (5,000 *g* for 10 min) and the supernatant was cleared by incubation (1 h) with 5 µl of preimmune rabbit serum. Protein agarose Ig A/G beads (10 µl; Autogen Bioclear) were added, and after 2 h, immunoprecipitated material was removed by centrifugation (1,000 *g* for 1 min). An aliquot (300 µl) of the cleared lysate was incubated with the primary antiserum (Table S1, available at http://www.jcb.org/cgi/content/full/jcb.200803172/DC1) for 1 h before addition of protein A/G–agarose beads (50 µl) and incubation for 12 h. After centrifugation (1,000 *g* for 1 min), the supernatant and pellet (washed three times) were used for WB. WB used 3–8% Tris acetate NuPAGE gels (Invitrogen), and blots were quantified using a GeneGnome (SynGene) with gel loadings adjusted to ensure that intensities scaled linearly with protein loading. Antibodies are listed in Table S1.

Quantitative PCR (QPCR)

cDNA was synthesized in a final volume of 20 µl directly from cell lysate using Fastlane cell cDNA kit (QIAGEN) according to the manufacturer's instructions. For QPCR, each reaction included primers specific for AC (Ludwig and Seuwen, 2002) or IP_3R subtypes (Quantitect Primer Assay; QIAGEN), and for calibration, primers for a house-keeping gene (GAPDH; Ogunwobi et al., 2006). Each reaction (25 µl) contained 1 µl of the HEK-PR1 reverse-transcription product, 0.5 µM of the AC- or IP_3R-specific primers, and Quantace Sensimix according to the manufacturer's instructions (Bioline). For PCR (Rotor-Gene 6000; Corbett Life Sciences), an initial denaturation at 93°C for 10 min was followed by 40 cycles of amplification (93°C for 10 s, 50–65°C for 15 s, and 72°C for 20 s). Expression levels were calculated as described previously (Moneer et al., 2005).

Quantification of signaling proteins

HEK-PR1 cells were washed in HBS supplemented with a complete protease inhibitor cocktail (Roche) and resuspended ($\sim 4 \times 10^6$ cells per milliliter) in TM (50 mM Tris and 1 mM EDTA, pH 8.3) for ^{3}H-IP_3 binding, in DM (75 mM Tris, 1 mM EDTA, 12.5 mM $MgCl_2$, and 0.2% BSA, pH 7.4) for ^{3}H-dihydroalprenolol (DHA) binding, and in FM (50 mM Tris and 10 mM $MgCl_2$, pH 7.4) for ^{3}H-FK binding. Cells were lysed (Polytron, Inc.), and the lysates were used for equilibrium competition binding assays. Incubations, in a final volume of 500 µl, included ^{3}H-IP_3 (1.5 nM, 21 Ci/mmol; PerkinElmer), ^{3}H-DHA (0.165 nM, 97 Ci/mmol; GE Healthcare), or ^{3}H-FK (10 nM, 27 Ci/mmol; PerkinElmer; with 100 µM p[NH]ppG, 10 µM isoproterenol, and 40 µM cytochalasin; Emala et al., 2000); each with appropriate concentrations of unlabeled competing ligand. After equilibrium had been attained (5 min on ice for ^{3}H-IP_3, 90 min at 25°C with shaking for ^{3}H-DHA, and 10 min at 25°C for ^{3}H-FK), incubations were terminated by centrifugation (20,000 *g* for 5 min at 4°C) and the pellet was washed with cold buffer, then resuspended in 200 µl of buffer for liquid scintillation counting. For ^{125}I-PTH binding, cells in 24-well plates ($2–5 \times 10^5$ cells per well) were incubated in PM (Dulbecco's modified Eagles medium with 20 mM Hepes and 0.1% BSA) with ^{125}I-PTH (44 pM, 1559 Ci/mmol; Bachem) for 5 h at 4°C (Chauvin et al., 2002). Cells were washed twice with ice-cold PBS and lysed with 0.8 M NaOH, then their radioactivity was determined. Equilibrium competition binding curves were fitted to four parameter logistic equations (GraphPad Prism; GraphPad Software) from which IC_{50} (and thence K_D) and B_{max} values were calculated. Expression of Gαs was quantified by WB, calibrated using recombinant Gαs (EMD).

Analysis

Concentration-effect relationships were individually fitted to four-parameter logistic equations by nonlinear curve-fitting (Prism 4; GraphPad Software), and the results from each experiment (EC_{50}, Hill coefficient *h*, and maximal response) were pooled for analyses. For simplicity, EC_{50} values are given as means ± SEM, although log EC_{50} values were used for statistical analysis. Student's *t* test, or a one-way analysis of variance test followed by a post hoc Bonferroni's test were used as was appropriate.

Online supplemental material

Fig. S1 shows that PTH potentiates Ca^{2+} signals by sensitizing IP_3R. Fig. S2 shows that potentiation of Ca^{2+} responses by isoproterenol and FK does not require PKA. Fig. S3 shows that inhibition of cAMP formation or degradation does not directly effect potentiation of Ca^{2+} responses by isoproterenol or FK. Fig. S4 shows the selectivity of the AC antibodies and the lack of

effect of AC3 or AC6 siRNA on CCh-evoked Ca^{2+} release. Table S1 lists the antibodies used. Online supplemental material is available at http://www.jcb.org/cgi/content/full/jcb.200803172/DC1.

We thank P. Marley, S. Yarwood, and G. Milligan for antisera to acetylated-cAMP, epac-1, and Gαs, respectively; and M. Falcke (Berlin) for advice on diffusion.

This work was supported by the Wellcome Trust (072084).

Submitted: 31 March 2008
Accepted: 22 September 2008

References

Baragli, A., M.L. Grieco, P. Trieu, L.R. Villeneuve, and T.E. Hebert. 2008. Heterodimers of adenylyl cyclases 2 and 5 show enhanced functional responses in the presence of Gαs. *Cell. Signal.* 20:480–492.

Behar, V., M. Pines, C. Nakamoto, Z. Greenberg, A. Bisello, S.M. Stueckle, R. Bessalle, T.E. Usdin, M. Chorev, M. Rosenblatt, and L.J. Suva. 1996. The human PTH2 receptor: binding and signal transduction properties of the stably expressed recombinant receptor. *Endocrinology.* 137:2748–2757.

Berridge, M.J. 1997. Elementary and global aspects of calcium signalling. *J. Physiol.* 499:291–306.

Bos, J.L. 2003. Epac: a new cAMP target and new avenues in cAMP research. *Nat. Rev. Mol. Cell Biol.* 4:733–738.

Bray, D. 1995. Protein molecules as computational elements in living cells. *Nature.* 376:307–312.

Brooker, G., J.F. Harper, W.L. Terasaki, and R.D. Moylan. 1979. Radioimmunoassay of cyclic AMP and cyclic GMP. *Adv. Cyclic Nucleotide Res.* 10:1–33.

Bruce, J.I.E., S.V. Straub, and D.I. Yule. 2003. Crosstalk between cAMP and Ca^{2+} signaling in non-excitable cells. *Cell Calcium.* 34:431–444.

Brummelkamp, T.R., R. Bernards, and R. Agami. 2002. A system for stable expression of short interfering RNAs in mammalian cells. *Science.* 296:550–553.

Buckley, K.A., S.C. Wagstaff, G. McKay, R.A. Hipskind, G. Bilbe, J.A. Gallagher, and W.B. Bowler. 2001. Parathyroid hormone potentiates nucleotide-induced $[Ca^{2+}]_i$ release in rat osteoblasts independently of G_q activation or cyclic monophosphate accumulation. *J. Biol. Chem.* 276:9565–9571.

Burgess, G.M., G.S.J. Bird, J.F. Obie, and J.W. Putney Jr. 1991. The mechanism for synergisms between phospholipase C- and adenylylcyclase-linked hormones in liver. *J. Biol. Chem.* 266:4772–4781.

Chauvin, S., M. Bencsik, T. Bambino, and R.A. Nissenson. 2002. Parathyroid hormone receptor recycling: role of receptor dephosphorylation and β-arrestin. *Mol. Endocrinol.* 16:2720–2732.

Christensen, A.E., F. Selheim, J. de Roooij, S. Dremier, F. Schwede, K.K. Dao, A. Martinez, C. Maenhaut, J.L. Bos, H.-G. Genieserm, and S.O. Døskeland. 2003. cAMP analog mapping of epac1 and cAMP kinase. Discriminating analogs demonstrate that Epac and cAMP kinase act syneristically to promote PC12 cell neurite extension. *J. Biol. Chem.* 278:35394–35402.

Di Biase, V., and C. Franzini-Armstrong. 2005. Evolution of skeletal type e-c coupling: a novel means of controlling calcium delivery. *J. Cell Biol.* 171:695–704.

Dodge-Kafka, K.L., J. Soughayer, G.C. Pare, J.J. Carlisle Michel, L.K. Langeberg, M.S. Kapiloff, and J.D. Scott. 2005. The protein kinase A anchoring protein mAKAP coordinates two integrated cAMP effector pathways. *Nature.* 437:574–578.

Dremier, S., R. Kopperud, S.O. Doskeland, J.E. Dumont, and C. Maenhaut. 2003. Search for new cyclic AMP-binding proteins. *FEBS Lett.* 546:103–107.

Dupont, G., G. Houart, and P. De Koninck. 2003. Sensitivity of CaM kinase II to the frequency of Ca^{2+} oscillations: a simple model. *Cell Calcium.* 34:485–497.

Dyachok, O., Y. Isakov, J. Sagetorp, and A. Tengholm. 2006. Oscillations in cyclic AMP in hormone-stimulated insulin-secreting β-cells. *Nature.* 439:349–352.

Emala, C.W., J. Clancy-Keen, and C.A. Hirshman. 2000. Decreased adenylyl cyclase protein and function in airway smooth muscle by chronic carbachol pretreatment. *Am. J. Physiol. Cell Physiol.* 279:C1008–C1015.

Fisher, D.A., J.F. Smith, J.S. Pillar, S.H. St Denis, and J.B. Cheng. 1998. Isolation and characterization of PDE8A, a novel human cAMP-specific phosphodiesterase. *Biochem. Biophys. Res. Commun.* 246:570–577.

Gorbunova, Y.V., and N.C. Spitzer. 2002. Dynamic interactions of cyclic AMP transients and spontaneous Ca^{2+} spikes. *Nature.* 418:93–96.

He, L.-P., N.M. Soldatov, and M. Morad. 2003. Molecular determinants of cAMP-mediated regulation of the Na^{+}-Ca^{2+} exchanger expressed in human cell lines. *J. Physiol.* 548:677–689.

Huang, X., H.M. Holden, and F.M. Raushel. 2001. Channeling of substrates and intermediates in enzyme-catalyzed reactions. *Annu. Rev. Biochem.* 70:149–180.

Jüppner, H., A.-B. Abou-Samra, M. Freeman, X.F. Kong, E. Schipani, J. Richards, L.F. Kolakowski, J. Hock, J.T. Potts, H.M. Kronenberg, and G.V. Segre. 1991. A G-protein-linked receptor for parathyroid hormone and parathyroid hormone-related peptide. *Science.* 254:1024–1026.

Law, S.F., K. Yasuda, G.I. Bell, and T. Reisine. 1993. Giα3 and Goα selectively associate with the cloned somatostatin receptor subtype SSTR2. *J. Biol. Chem.* 268:10721–10727.

Ludwig, M.-G., and K. Seuwen. 2002. Characterization of the human adenylyl cyclase gene family: cDNA, gene structure, and tissue distribution of the nine isoforms. *J. Recept. Signal Transduct. Res.* 22:79–110.

Luik, R.M., M.M. Wu, J. Buchanan, and R.S. Lewis. 2006. The elementary unit of store-operated Ca^{2+} entry: local activation of CRAC channels by STIM1 at ER-plasma membrane junctions. *J. Cell Biol.* 174:815–825.

Mahon, M.J., T.M. Bonacci, P. Divieti, and A.V. Smrcka. 2006. A docking site for G protein βγ subunits on the parathyroid hormone 1 receptor supports signaling through multiple pathways. *Mol. Endocrinol.* 20:136–146.

Marley, P.D., K.A. Thomson, K. Jachno, and M.J. Johnston. 1991. Histamine-induced increases in cyclic AMP levels in bovine adrenal medullary cells. *Br. J. Pharmacol.* 104:839–846.

Moneer, Z., I. Pino, E.J.A. Taylor, L.M. Broad, Y. Liu, S.C. Tovey, L. Staali, and C.W. Taylor. 2005. Different phospholipase-C-coupled receptors differentially regulate capacitative and non-capacitative Ca^{2+} entry in A7r5 cells. *Biochem. J.* 389:821–829.

Mongillo, M., C.G. Tocchetti, A. Terrin, V. Lissandron, Y.F. Cheung, W.R. Dostmann, T. Pozzan, D.A. Kass, N. Paolocci, M.D. Houslay, and M. Zaccolo. 2006. Compartmentalized phosphodiesterase-2 activity blunts β-adrenergic cardiac inotropy via an NO/cGMP-dependent pathway. *Circ. Res.* 98:226–234.

Ogunwobi, O., G. Mutungi, and I.L. Beales. 2006. Leptin stimulates proliferation and inhibits apoptosis in Barrett's esophageal adenocarcinoma cells by cyclooxygenase-2-dependent, prostaglandin-E2-mediated transactivation of the epidermal growth factor receptor and c-Jun NH2-terminal kinase activation. *Endocrinology.* 147:4505–4516.

Olveczky, B.P., and A.S. Verkman. 1998. Monte Carlo analysis of obstructed diffusion in three dimensions: application to molecular diffusion in organelles. *Biophys. J.* 74:2722–2730.

Penn, R.B., J.L. Parent, A.N. Pronin, R.A. Panettieri Jr., and J.L. Benovic. 1999. Pharmacological inhibition of protein kinases in intact cells: antagonism of β adrenergic receptor ligand binding by H-89 reveals limitations of usefulness. *J. Pharmacol. Exp. Ther.* 288:428–437.

Reid, I.R., C. Lowe, J. Cornish, D.H. Gray, and S.J.M. Skinner. 1990. Adenylate cyclase blockers dissociate PTH-stimulated bone resorption from cAMP production. *Am. J. Physiol.* 258:E708–E714.

Rich, T.C., K.A. Fagan, H. Nakata, J. Schaak, D.M.F. Cooper, and J.W. Karpen. 2000. Cyclic nucleotide-gated channels colocalize with adenylyl cyclase in regions of restricted cAMP diffusion. *J. Gen. Physiol.* 116:147–161.

Schmidt, M., S. Evellin, P.A.O. Weernink, F. vom Dorp, H. Rehmann, J.W. Lomasney, and K.H. Jakobs. 2001. A new phospholipase-C-calcium signalling pathway mediated by cyclic AMP and a Rap GTPase. *Nat. Cell Biol.* 3:1020–1024.

Screaton, R.A., M.D. Conkright, Y. Katoh, J.L. Best, G. Canettieri, S. Jeffries, E. Guzman, S. Niessen, J.R.I. Yates, H. Takemori, et al. 2004. The CREB coactivator TIRC2 functions as a calcium- and cAMP-sensitive coincidence detector. *Cell.* 119:61–74.

Seuwen, K., and H.G.W.M. Boddeke. 1995. Heparin-insensitive calcium release from intracellular stores triggered by the recombinant human parathyroid hormone receptor. *Br. J. Pharmacol.* 114:1613–1620.

Short, A.D., and C.W. Taylor. 2000. Parathyroid hormone controls the size of the intracellular Ca^{2+} stores available to receptors linked to inositol trisphosphate formation. *J. Biol. Chem.* 275:1807–1813.

Smith, F.D., L.K. Langeberg, and J.D. Scott. 2006. The where's and when's of kinase anchoring. *Trends Biochem. Sci.* 31:316–323.

Soulsby, M.D., and R.J. Wojcikiewicz. 2007. Calcium mobilization via type III inositol 1,4,5-trisphosphate receptors is not altered by PKA-mediated phosphorylation of serines 916, 934, and 1832. *Cell Calcium.* 42:261–270.

Straub, S.V., D.R. Giovannucci, J.I.E. Bruce, and D.I. Yule. 2002. A role for phosphorylation of inositol 1,4,5-trisphosphate receptors in defining calcium signals induced by peptide agonists in pancreatic acinar cells. *J. Biol. Chem.* 277:31949–31956.

Strickland, S., and J.N. Loeb. 1981. Obligatory separation of hormone binding and biological response curves in systems dependent upon secondary mediators of hormone action. *Proc. Natl. Acad. Sci. USA.* 78:1366–1370.

Takasu, H., T.J. Gardella, M.D. Luck, J.T. Potts, and F.R. Bringhurst. 1999. Amino-terminal modifications of human parathyoid hormone (PTH) selectively alter phospholipase C signaling via the type 1 PTH receptor: Implications for design of signal-specific PTH ligands. *Biochemistry.* 38:13453–13460.

Tovey, S.C., T.A. Goraya, and C.W. Taylor. 2003. Parathyroid hormone increases the sensitivity of inositol trisphosphate receptors by a mechanism that is independent of cyclic AMP. *Br. J. Pharmacol.* 138:81–90.

Tovey, S.C., Y. Sun, and C.W. Taylor. 2006. Rapid functional assays of intracellular Ca^{2+} channels. *Nat. Protocols.* 1:259–263.

Treves, S., C. Franzini-Armstrong, L. Moccagatta, C. Arnoult, C. Grasso, A. Schrum, S. Ducreux, M.X. Zhu, K. Mikoshiba, T. Girard, et al. 2004. Junctate is a key element in calcium entry induced by activation of $InsP_3$ receptors and/or calcium store depletion. *J. Cell Biol.* 166:537–548.

Varnai, P., B. Toth, D.J. Toth, L. Hunyady, and T. Balla. 2007. Visualization and manipulation of plasma membrane-endoplasmic reticulum contact sites indicates the presence of additional molecular components within the STIM1-Orai1 Complex. *J. Biol. Chem.* 282:29678–29690.

Werry, T.D., G.F. Wilkinson, and G.B. Willars. 2003. Mechanisms of cross-talk between G-protein-coupled receptors resulting in enhanced release of intracellular Ca^{2+}. *Biochem. J.* 374:281–296.

Willoughby, D., and D.M. Cooper. 2007. Organization and Ca^{2+} regulation of adenylyl cyclases in cAMP microdomains. *Physiol. Rev.* 87:965–1010.

Willoughby, D., W. Wong, J. Schaack, J.D. Scott, and D.M. Cooper. 2006. An anchored PKA and PDE4 complex regulates subplasmalemmal cAMP dynamics. *EMBO J.* 25:2051–2061.

Willoughby, D., G.S. Baillie, M.J. Lynch, A. Ciruela, M.D. Houslay, and D.M. Cooper. 2007. Dynamic regulation, desensitization and crosstalk in discrete sub-cellular microdomains during β2-adrenoceptor and prostanoid receptor cAMP signalling. *J. Biol. Chem.* 282:34235–34249.

Wojcikiewicz, R.J.H. 1995. Type I, II and III inositol 1,4,5-trisphosphate receptors are unequally susceptible to down-regulation and are expressed in markedly different proportions in different cell types. *J. Biol. Chem.* 270:11678–11683.

Wong, W., and J.D. Scott. 2004. AKAP signalling complexes: focal points in space and time. *Nat. Rev. Mol. Cell Biol.* 5:959–970.

Zaccolo, M., and T. Pozzan. 2002. Discrete microdomains with high concentrations of cAMP in stimulated rat neonatal cardiac myocytes. *Science.* 295:1711–1715.

Zeng, W., D.D. Mak, Q. Li, D.M. Shin, J.K. Foskett, and S. Muallem. 2003. A new mode of Ca^{2+} signaling by G protein-coupled receptors: gating of IP_3 receptor Ca^{2+} release channels by Gβγ. *Curr. Biol.* 13:872–876.

Zerr, P., U. Becherer, J.L. Rodeau, and A. Feltz. 1996. Forskolin's structural analogue 1,9-dideoxyforskolin has Ca^{2+} channel blocker-like action in rat cerebellar granule cells. *Eur. J. Pharmacol.* 303:101–108.